Enhancing Microbial Fuel Cell (MFC) Activity by Incorporating Polypyrrole/MXene Composite as an Anode Material

By

Fareeha Batool

(Registration No: 00000400952)

Department of Materials Engineering

School of Chemical and Materials Engineering

National University of Sciences & Technology (NUST)

Islamabad, Pakistan

(2024)

Enhancing Microbial Fuel Cell (MFC) Activity by Incorporating Polypyrrole/MXene Composite as an Anode Material

By

Fareeha Batool

(Registration No: 00000400952)

A thesis submitted to the National University of Sciences and Technology, Islamabad,

in partial fulfillment of the requirements for the degree of

Master of Science in
Nanoscience and Engineering

Supervisor: Dr. Usman Liaqat

School of Chemical and Materials Engineering

National University of Sciences & Technology (NUST)

Islamabad, Pakistan

(2024)

THESIS ACCEPTANCE CERTIFICATE

THESIS ACCEPTANCE CERTIFICATE

Certified that final copy of MS thesis written by Ms **Fareeha Batool** (Registration No 00000400952), of School of Chemical & Materials Engineering (SCME) has been vetted by undersigned, found complete in all respects as per NUST Statues/Regulations, is free of plagiarism, errors, and mistakes and is accepted as partial fulfillment for award of MS degree. It is further certified that necessary amendments as pointed out by GEC members of the scholar have also been incorporated in the said thesis.

Signature: _____

Name of Supervisor: <u>Dr Usman Liaqat</u>

Date: <u>31-07-24</u>

Signature (HOD): _____

Date: _____ 3/7/24

Signature (Dean/Principal): _____ 1/8/24

Date: _____

TH - 1

NISE-10-2022 **Form TH-1**

National University of Sciences & Technology (NUST)

MASTER'S THESIS WORK

Formulation of Guidance and Examination Committee (GEC)

ame: Fareeha Batool   NUST Reg No: 00000400952

epartment: Department of Materials Engineering   Specialization: Master of Science in Nanoscience & Engineering

edit Hour Completed: 24.0   CGPA: 4.0

Course Work Completed

S/No:	Code:	Title:	Core/Elective:	CH:	Grade:
1.	MSE-854	Characterization Of Materials	Compulsory	3.0	A
2.	NSE-813	Essentials of Nanoscience and Engineering	Compulsory	3.0	A
3.	RM-898	Research Methodology	Additional	2.0	Q
4.	NSE-843	Nano Technology And Photovoltaics	Elective	3.0	A
5.	MSE-856	Nano Material and Processing	Compulsory	3.0	A
6.	NSE-941	Nano Composite Materials	Elective	3.0	A
7.	MSE-952	Materials For Biomedical Applications	Elective	3.0	A
8.	MSE-954	Advanced Characterization Techniques	Elective	3.0	A
9.	ESE-837	Electrochemical Energy Storage and Conversion	Elective	3.0	A

ate 10 - Dec - 2023   Student's Signature

Thesis Committee

Name: Usman Liaqat (Supervisor)   Signature
Department: Department of Materials Engineering

Name: Waheed Miran (Cosupervisor)   Signature
Department: Department of Chemical Engineering

Name: Muhammad Bilal Khan Niazi (Internal)   Signature
Department: Department of Chemical Engineering

Name: Syed Rizwan Hussain (Internal)   Signature
Department: Department of Physics

ite: 10 - Dec - 2023   Signature of Head of Department:

APPROVAL

ite: 10 - Dec - 2023   Signature of Dean/Principal:

School of Chemical & Materials Engineering (SCME) H-12 Campus,

TH – 4

National University of Sciences &Technology (NUST)

MASTER'S THESIS WORK

We hereby recommend that the dissertation prepared under our supervision by

Regn No & Name: <u>00000400952 Fareeha Batool</u>

Title: <u>Enhancing Microbial Fuel Cell (MFC) Activity by Incorporating Polypyrrole/MXene Composite as an Anode Material.</u>

Presented on: <u>11 Jul 2024</u>   at: <u>1430 hrs in SCME (Seminar Hall)</u>

Be accepted in partial fulfillment of the requirements for the award of Masters of Science degree in **Nanoscience & Engineering.**

Guidance & Examination Committee Members

Name: **Dr Muhammad Bilal Khan Niazi**   Signature: _____

Name: **Dr Syed Rizwan Hussain** (External)   Signature: _____

Name: **Dr Waheed Miran** (Co-Supervisor)   Signature: _____

Supervisor's Name: <u>Dr Usman Liaqat</u>   Signature: _____

Dated: 29.07.24

Head of Department
Date 29/7/24

Dean/Principal
Date 30/7/24

School of Chemical &Materials Engineering (SCME)

AUTHOR'S DECLARATION

I Fareeha Batool hereby state that my MS thesis titled "Enhancing Microbial Fuel Cell (MFC) Activity by Incorporating Polypyrrole/MXene Composite as an Anode Material" is my own work and has not been submitted previously by me for taking any degree from National University of Sciences and Technology, Islamabad or anywhere else in the country/ world.

At any time if my statement is found to be incorrect even after I graduate, the university has the right to withdraw my MS degree.

Name of Student: Fareeha Batool

Date: 10 June 2024

PLAGIARISM UNDERTAKING

I solemnly declare that research work presented in the thesis titled "Enhancing Microbial Fuel Cell (MFC) Activity by Incorporating Polypyrrole/MXene Composite as an Anode Material" is solely my research work with no significant contribution from any other person. Small contribution/ help wherever taken has been duly acknowledged and that complete thesis has been written by me.

I understand the zero-tolerance policy of the HEC and National University of Sciences and Technology (NUST), Islamabad towards plagiarism. Therefore, I as an author of the above titled thesis declare that no portion of my thesis has been plagiarized and any material used as reference is properly referred/cited.

I undertake that if I am found guilty of any formal plagiarism in the above titled thesis even after award of MS degree, the University reserves the rights to withdraw/revoke my MS degree and that HEC and NUST, Islamabad has the right to publish my name on the HEC/University website on which names of students are placed who submitted plagiarized thesis.

Student Signature: _____

Name: Fareeha Batool

DEDICATION

"Dedicated to Almighty Allah, my supervisor and my beloved family. It could not have been possible without them."

ACKNOWLEDGEMENTS

TABLE OF CONTENTS

LIST OF TABLES

LIST OF FIGURES

LIST OF SYMBOLS, ABBREVIATIONS AND ACRONYMS

EDX	Energy Dispersive X-Ray
SEM	Scanning Electron Microscope
XRD	X-ray Powder Diffraction
FTIR	Fourier-Transform Infrared Spectroscopy
MFC	Microbial Fuel Cell
nm	Nanometers
PPy	Polypyrrole
EET	Extracellular electron transfer
MXene	Ti_3C_2
MAX	Ti_3AlC_2

ABSTRACT

Microbial fuel cells (MFC) have been recognized as a promising green and clean electricity generation device. The anode is critical to the electricity generation process within MFC. Microbes in the anodic chamber oxidize organic substrates, releasing protons and electrons in the process. These electrons are subsequently transferred to the anode surface, where they generate an electric current. When protons from the anode pass through a proton exchange membrane (PEM) and electrons passing from external circuit combine with oxygen to form water at cathode, the electrochemical circuit is completed. Improving MFC performance using MXene (Ti_3C_2) as anode material is a promising method. MXene is a material with a large surface area and tunable chemical properties. Our goal is to maximize the catalytic capabilities of MXene layers to improve the efficiency of MFCs by depositing it on the anode surface and speeding up electron transmission. For this, Polypyrrole (PPy) can boost the redox activity, stability and conductivity of the electrode surface. The Polypyrrole/MXene composite adds a new dimension to this research. Hydrofluoric acid (HF) etching approach is being used to exfoliate MXene sheets, followed by in-situ polymerization of pyrrole to generate a PPy/MXene composite. The MFC fabricated with as prepared PPy/MXene@GF anode had the highest power density of 264 mW/m^2 and a maximum output voltage of 281 mV, then that of MXene@GF (197 mW/m^2, 157 mV) and unmodified Graphite felt (GF) (45 mW/m^2, 101 mV). This improved performance can be attributed to the material's reduced charge transfer resistance (R_{ct}) and solution resistance (R_s) combined with higher bacterium affinity, resulting in increased extracellular electron transfer (EET) efficiency. This study shows that the PPy/MXene composite possesses good potential as an anode in terms of MFC power generation.

Keywords: Microbial fuel cell (MFC), Anode material, PPy/MXene composite, Microbial community, Extracellular electron transfer (EET), Power density.

GRAPHICAL ABSTRACT
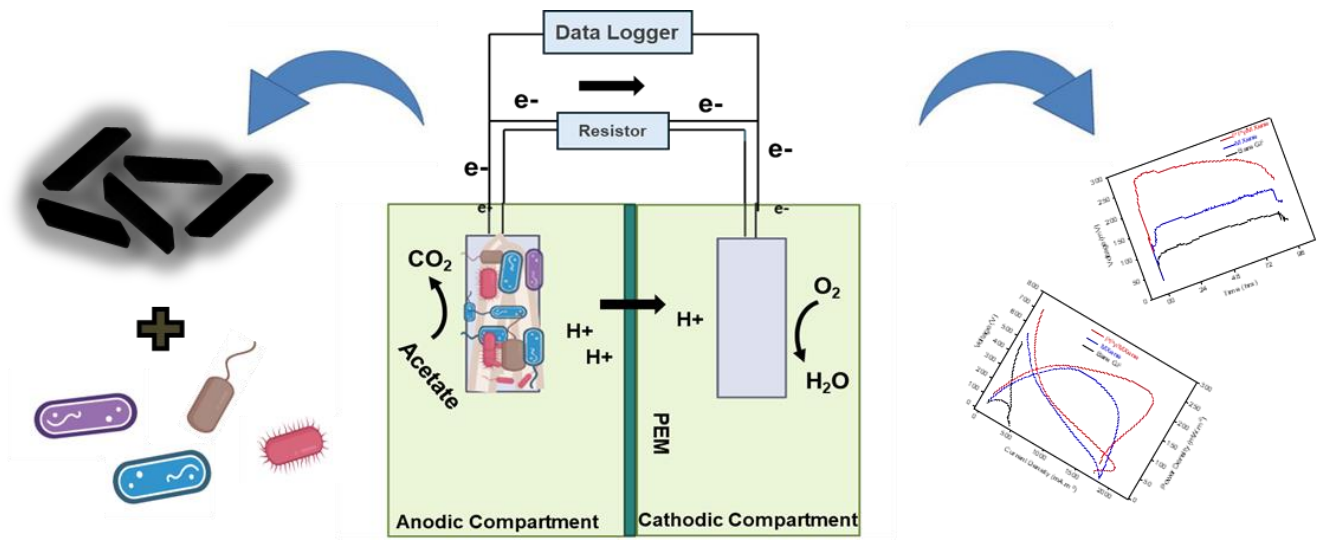
CHAPTER 1: INTRODUCTION

This thesis focuses on sustainable energy production, incorporating titanium carbide MXene ($Ti_3C_2T_x$) to Microbial Fuel Cells (MFCs) for boosting bioelectricity output. This study has focused upon the anode modifier properties of MXene and its composite with polypyrrole (PPy). The purpose of this study is to understand the mutually advantageous link between microbial electrochemistry and MXene-based structures to develop sustainable energy harvesting techniques.

1.1 Background

The scientific community has been interested in microbial fuel cell (MFC) technology for the last ten to fifteen years due to the possibility for directly turning organic waste into electricity via various processes as through enzymatic, microbial and photosynthetic algae breakdown and generating current involving electrochemical reactions [1]. The first MFCs were proven in the early twentieth century with the use of a mediator, a chemical that transports electrons from the bacteria to the anode in the cell. Unmediated MFCs originally debuted in the 1970s; in these MFCs, bacteria typically have cytochromes or other electrochemically active redox proteins on their outer membranes, allowing them to send electrons directly to the anodes. Commercially, MFC used in wastewater treatment started in the twenty-first century [2].

The primary worldwide challenges of increased energy consumption, water scarcity, and climate change have highlighted the urgent need for the development of clean and sustainable technology. MFCs use bacteria's natural metabolic ability to convert organic resources into electrical energy. This approach not only addresses the linked issues of carbon emissions and wastewater purification, but it also makes it easier to produce sustainable energy [3]. According to a study, MFCs may remove up to 80% of the organic material found in sewage effluent. Aside from the necessity to pretreat the water to remove toxins, the technique is quite similar to that of treating brewery effluent. This is a tough stage since the composition of sewage effluent varies significantly and before filling into MFC, it may require prolong treatment. Nonetheless, the electricity

created during the wastewater treatment process warrants such extensive treatment. MFC-generated power will help to reduce the highly expensive wastewater treatment process [3].

This thesis aims to contribute to current knowledge by investigating the various advantages and disadvantages of using MXene-based anodes in MFC. It investigates the possibilities of MXene-based anodes in terms of bioelectricity generation and related applications. It will accomplish this by thoroughly reviewing the literature, experimental data, and theoretical issues.

1.2   A Brief History

In 1911, University of Durham botany professor M. C. Potter came up with the concept of using microbes to produce energy. During his research on the breakdown of organic molecules by microorganisms, he also found that electricity was generated. Potter came up with the plan to try to extract this recently discovered energy source for human usage. Although he was able to build a crude microbial fuel cell, the concept could not be further enhanced because insufficient knowledge about bacterial metabolism was available [4]. The design of the first microbial fuel cell was reinvented by M. J. Allen and H. Peter Bennetto of Kings College in London. Driven by their aspiration to furnish affordable and dependable energy to developing nations, Allen and Bennetto integrated substantial technological breakthroughs with growing comprehension of the electron transport chain to generate the fundamental blueprint being employed in MFCs today. One key mystery persisted as researchers into the microbial fuel cell spread throughout the globe: how can electrons move from the electron transport chain to the anode? B-H. Kim of the Korean Institute of Science and Technology found that some bacteria were electrochemically active, and they don't need mediator molecules for transferring electrons to the electrodes when investigating this issue in the 1990s. Consequently, the need for expensive and occasionally hazardous mediators was removed with the introduction of a novel kind of microbial fuel cell. Researchers are currently attempting to maximize electron transfer, bacterial species and combinations, and electrode materials in microbial fuel cells. Although the concept of using bacteria to produce energy has been

around for over a century, scientists are still learning everything there is to know about the MFC and how to fully realize its potential.

1.3 Construction & Working Principle

The essential components of a microbial fuel cell (MFC) are the anode chamber, cathode chamber, electrodes, and a proton exchange membrane (PEM) or salt bridge. The anode chamber contains an organic substrate, such as soil or wastewater, that has been injected with anaerobic bacteria to enhance the oxidation of organic molecules. The anode electrode is often made of carbon cloth or graphite. The cathode electrode, which is likewise composed of conductive materials like graphite or carbon cloth, is placed in the cathode chamber, which is also supplied with oxidizing agents or aerated water to aid in the reduction reaction. By dividing the two chambers and keeping their contents from mixing, the PEM permits protons to move from the anode to the cathode. The electrodes are wired to an external circuit that has a multimeter for measuring electrical output, a resistor or load, and other components. While the cathode chamber is kept aerobic to promote effective electron transfer and energy generation, the anode chamber is kept anaerobic to maximize microbial activity [5].

When bacteria in the anode chamber digest organic substrates, microbial oxidation begins. During this metabolic activity, the microbial respiratory chain produces byproducts that include electrons. Typically, an electron acceptor inside the microbial cell receives the electrons during the conventional process of cellular respiration (Fig.1.1). However, in MFC, the microbial cells purposefully lack an external electron acceptor, which causes the release of electrons into the extracellular environment. Released electrons go through the conductive anode structure, which is frequently made of materials like graphite or carbon fiber and form an electrically conductive biofilm on the anode's surface. Electrical biofilm serves as a medium between microorganisms. Parallel to this, a comparable oxidation-reduction reaction occurs in the cathode chamber. Commonly used cathodic electron acceptors include oxygen or other oxidizing agents. The electrochemical circuit is completed at the cathode when electrons from the external circuit react with protons and the cathodic electron acceptor to produce water or other reduced molecules [6]. The overall chemical reaction is as follows:

At the Anode:

Organic matter (substrate) → Microbial oxidation + Release of electrons

At the Cathode:

Electrons from anode + Cathodic electron acceptor + Protons → Formation of water or reduced compounds
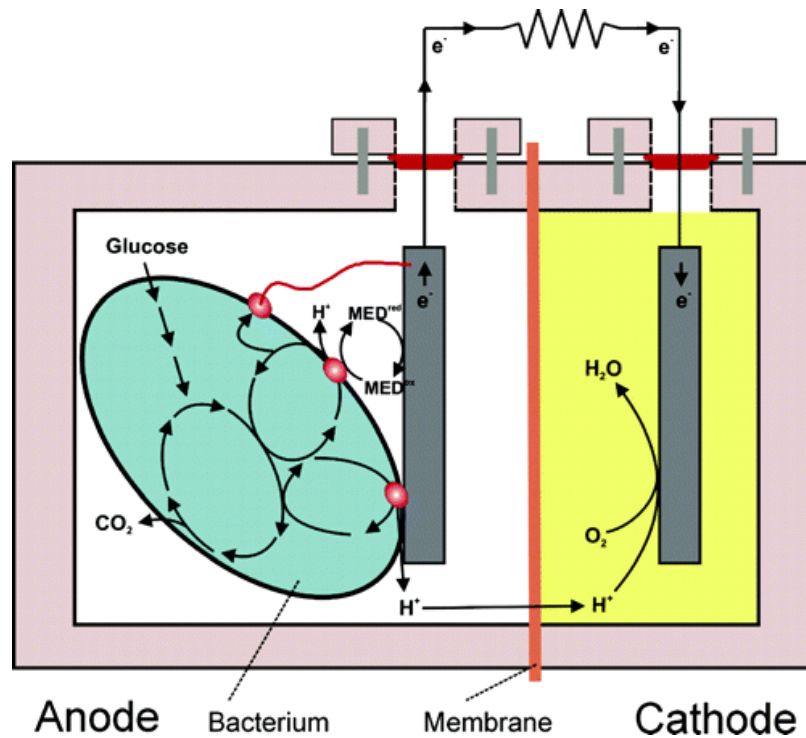
Figure 1.1: Construction & working of MFC [7]

1.4 MXene

MXene represents a class of two-dimensional (2D) materials consisting of carbonitrides, nitrides, or carbides of transition metals. In 2011, Drexel University researchers made the initial discovery of them. Their structure gives rise to the name "MXene". "M" stands for a transition metal, "X" for carbon or nitrogen, and "ene" for their resemblance to graphene [8]. The elements "A" from group 13 or 14 of the periodic table, "X" being carbon or nitrogen, and "M" being an early transition metal are the building blocks of layered MAX phases, which give rise to MXene. The general formula for

4

MXene is $M_{n+1}X_n$, where n = 1, 2, or 3. MXene has an excellent record of electrical conductivity. Because of this feature, it can be employed in conductive inks, batteries, and supercapacitors, and among other electronic applications. Unlike graphene, MXene is hydrophilic due to its surface terminations (such as -OH, -O, and -F). This property enhances its interaction with other molecules and ions, as well as its dispersion in aqueous solutions. It is possible to functionalize the surface of MXene with various groups (such as -OH, -O, or -F), giving them distinct chemical properties. This property allows MXene to be customized for specific tasks, such as environmental cleanup, energy storage, energy conversion, sensing, and catalysis [9].

1.5   Polypyrrole (PPy)

Pyrrole monomers are polymerized to form polypyrrole (PPy), a conductive polymer. Pyrrole is an aromatic heterocyclic compound containing five components. PPy is a highly explored conducting polymer due to its stability, electrical conductivity, and ease of production. The conjugated backbone structure of polypyrrole is responsible for its electrical conductivity. The standard chemical formula is $(C_4H_3NH)_n$, with the pyrrole units united in a chain through carbon-carbon bonds [10]. PPy exhibits significant electrical conductivity and can be modified chemically or by doping with various anions. Thin films or coatings of PPy can be deposited, offering mechanical flexibility that is useful in a variety of applications. PPy ability to undergo reversible redox processes makes it suitable for energy conversion and storage applications. PPy can be added to the electrode materials or as a catalyst support in fuel cells, batteries and supercapacitors increasing the overall efficiency and catalytic activity. These properties make PPy a promising material for advancing energy storage and conversion technologies.

1.6   Problem Statement

Microbial fuel cell (MFC) technology has captured the attention of the scientific community in the last 10 to 15 years for the possibility of transforming organic waste directly into electricity via various processes as through enzymatic, microbial and photosynthetic algae breakdown and producing current by involving electrochemical reactions. But still there are many issues as low power output, slow reaction rate, low

energy conversion efficiency and ineffective interaction between anode and electroactive microbes which create a bottleneck in their scaling up for commercial use. Despite these shortcomings, ongoing research and development efforts are aimed at improving MFC technology and addressing these limitations. Innovations in materials, microbial engineering, and system design may lead to broader and more practical applications for microbial fuel cells in the future. My aim is also towards developing such a composite material which can help in moving one step forward in overcoming all these above-mentioned constraints and increasing the overall performance of MFCs.

1.7   Objectives

- Successful synthesis of the MXene as an anodic material.

- Optimal synthesis of the composite of MXene as an anodic material.

- Increasing interaction between microorganisms and the modified anode therefore boosting the electron transfer mechanism

- Improvement in the power output/current density of MFC

CHAPTER 2: LITERATURE REVIEW

2.1   Microbial Fuel Cells (MFCs): A Brief Introduction

Microbial Fuel Cells (MFCs), which have lately expanded into diverse Bio-Electrochemical Systems (BESs), are an intriguing and quickly emerging branch of research and technology that combines classical abiotic electrochemical reactions and physics with biological catalytic redox activity [1]. Over the past 20 years, a great deal of knowledge has been gained about MFCs through a variety of activities, including studies on the biochemical and physical properties of the electron transport chain and electrochemically active bacteria used in mediator-less MFC systems, microbial communities, potential uses for this technology, different MFC configurations and designs, different types of construction and materials, and methods for data analysis and reporting to inform MFC developers [11], a comparison of the technologies of conventional anaerobic digestion and MFCs as well as the potential of the MFC systems as a complement to the anaerobic digestion technology [12], performances and optimization of the MFC systems' operating parameters [11], anodic electron transfer processes, various substrates used in MFCs, challenges associated with the MFC technology, and various electrode materials and designs for the cathode and anode sides [13, 14]. Although the concept of using bacteria to produce energy has been around for over a century, scientists are still learning everything there is to know about the MFC and how to fully realize its potential. In terms of modern MFC advances, [11] Bruce E. Logan's group belonged to Pennsylvania State University in the United States is regarded as a pioneer [3, 15, 16]. A few more notable organizations that have been making important advances in the field of MFCs are Lovely [17], Rabaey [18], Schroder [19], and others.

2.2   MFCs Main Components

The primary MFC elements that affects its performance are included in Table 1 and are briefly explained below:

2.2.1 Electrodes (Anode and Cathode)

In microbial fuel cells (MFCs), the anode and cathode are crucial components that facilitate the conversion of chemical energy into electrical energy through microbial activity. The anode is where oxidation occurs, with microorganisms metabolizing organic substrates and releasing protons and electrons. These electrons travel to acceptor where reduction reactions take place, often involving oxygen as the electron acceptor, and it combines with the electrons from external circuit and protons passing through membrane to form water. At the anode, typically the metabolic activity of microbes to produce sustainable electricity from organic waste materials occurs. High specific surface area, high porosity, biocompatibility, chemical stability, and high electrical conductivity anode materials function well in MFCs [20, 21]. All the materials used as an anode can be utilized as a cathode. The most common types of cathodes used in MFCs include platinum catalyst coated carbon, carbon without platinum catalyst, metals other than platinum and plain carbon.

2.2.2 Anolytes and Catholytes

The electrolytes found in the anode and cathode compartments of MFC are known as anolytes and catholytes, respectively. They are essential to the MFC's general functionality and efficiency because they make it easier for ions to move between the electrodes. Anodic chamber biology is the primary focus of MFC phenomena. In MFC, a variety of anolytes are employed, each containing a unique combination of mixed or pure culture exoelectrogens [22]. Additionally, research on MFC indicates the use of different substrates and biofilm electrodes, which combine to enhance performance in areas like power density and current density. Glucose, lactate, acetate, starch, sodium formate, municipal wastewater, artificial wastewater, etc. are some of the substrate varieties employed in MFCs. These substrates break down to release protons and electrons when they encounter the right electroactive bacteria, called inoculums. The majority of MFC research has made extensive use of oxygen as a catholyte and electron acceptor due to its abundant supply and high standard redox potential. In two chambered MFCs, ferricyanide,

8

potassium permanganate, or manganese dioxide can also be employed as cathodic electron acceptors.

2.2.3 Electrode Catalyst

An electrode catalyst is a substance used in MFCs that speeds up the electrochemical reactions taking place at the electrodes, increasing the fuel cell's overall efficiency. Catalysts at the anode aid in the oxidation of organic compounds by microorganisms, facilitating the flow of electrons to the electrode from the microbes. Catalysts usually work at the cathode to reduce oxygen (or other terminal electron acceptors) faster by accelerating electron transport and lowering the overpotential needed for the reaction. Various metal oxides, carbon-based compounds, and platinum are examples of common electrode catalysts. These materials are chosen for their capacity to boost electrical conductivity and reaction speeds without being wasted.

2.2.4 Ion (Proton) Exchange Membrane

In order for electrons to flow from the external circuit and produce electricity, protons must be transported from the anode to the cathode in MFCs via the proton exchange membrane (PEM) [23]. It maintains different electrochemical conditions that are essential for microbial activity and reduction processes by separating the anolyte and catholyte. By reducing ionic resistance and cross-contamination, the PEM improves stability and overall efficiency. The PEM is essential for extending the life and performance of MFCs because it keeps the ideal conditions for microbial development and electrochemical activities.

Table 2.1: Basic components of MFCs [4, 7, 24]

Items	Material
Anode	Graphite felt (GF), Carbon paper (CP), Carbon cloth (CC), Pt black, Pt, Graphite, Reticulated vitreous carbon (RVC)

Cathode	Graphite felt (GF), Carbon mesh (CM), Carbon cloth (CC), Pt, Nickel foam (NF)
Anodic compartment	Polycarbonate, Plexiglas, Glass
Cathodic compartment	Polycarbonate, Plexiglas, Glass
Proton exchange membrane (PEM)	Ultrex, Salt brodge, Nafion, Polyethylene, Porcelain septum, poly (styrene-co-divinylbenzene)
Electrode catalyst	Pt black, Fe^{+3}, Pt, Polyaniline (PANI), MnO_2

2.3   Basic Operating Principle of MFCs

Using organic materials in MFCs, bacteria can operate as a biocatalyst to create electrons in an anaerobic environment. Anaerobic anode section and aerobic cathode section are its two typical sections. An ion exchange membrane (also known as a proton exchange membrane) or salt bridge divides the two portions. In the anodic chamber, organic materials undergo oxidation, producing protons and electrons in the process [25]. Current is produced when electrons are supplied to the anode and travel through an external circuit. Protons enter the cathodic chamber, where they interact with oxygen to form water, after passing via a PEM or a salt bridge (Fig.2.1).

The chemical reactions that occur in different electrodes are detailed here, using glucose as an example of the primary substrate.

(1) Anode: $C_6H_{12}O_6 + 6H_2O \xrightarrow{bioelectricity} 24e- + 24H+ + 6CO_2$

(2) Cathode: $24e- + 24H+ + 6O_2 \longrightarrow 6H_2O$

(3) Overall reaction: $C_6H_{12}O_6 + 6O_2 \longrightarrow 6CO_2 + 6H_2O$
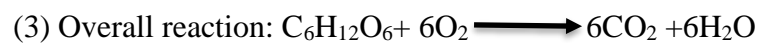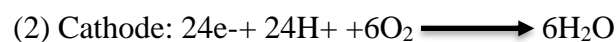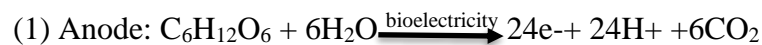
The substrate is broken down into carbon dioxide and water during the entire process, and energy is produced as a byproduct at the same time.
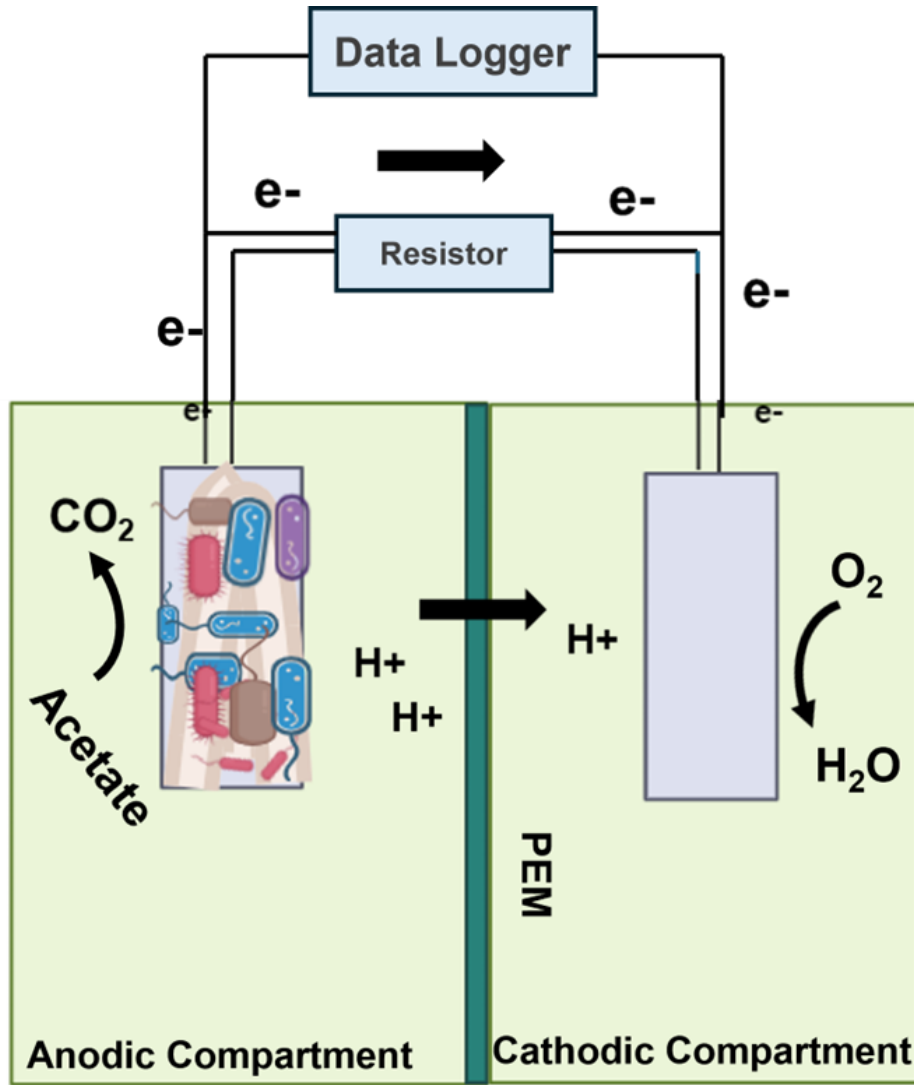
Figure 2.1: Basic operating principal schematic illustration for MFC.

2.4   MFC Reactor Types

MFC reactors come in many varieties, but they all essentially operate according to the same principles. Several designs and arrangements have been developed to maximize the integration of the three fundamental components as the separator, cathode, and anode into a functional system. The design of MFCs has a major impact on their performance. Frequently utilized types are succinctly defined as follows:

11

2.4.1 Single Chamber MFC

There is no need for a separate cathode chamber when using a single-chambered microbial fuel cell (SCMFC), as the cathode and anode are situated inside the same compartment. The anode of SCMFCs is normally immersed in an anolyte that contains microorganisms and organic substrates that are broken down by the organisms to produce protons and electrons (Fig.2.2) Electricity is produced as the electrons move from the cathode via an external circuit [3, 26]. The cathode aids in the reduction of oxygen or other electron acceptors and is frequently exposed to air or submerged in a catholyte. However, possible oxygen transfer from the cathode to the anode creates barriers and limits the efficiency of the electrochemical reactions. By using air cathodes with hydrophobic barriers to reduce oxygen passage, significant progress has been made in addressing these issues.
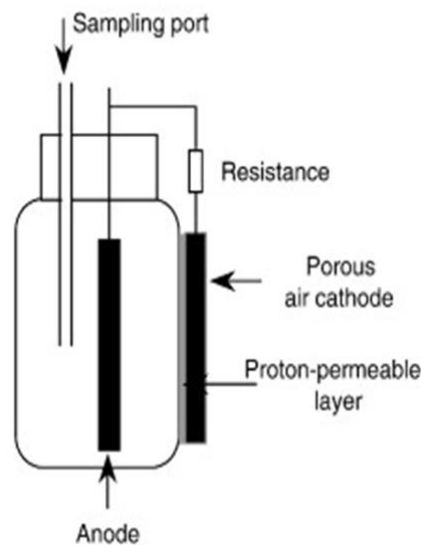
Figure 2.2: Single chamber MFC (SCMFC) [12]

2.4.2 Double Chamber MFC

Utilizing the metabolic processes of microorganisms in two distinct chambers an anode chamber with microbes and organic substrate and a cathode chamber with an electron acceptor, typically oxygen, divided by a proton exchange membrane (PEM), double chambered Microbial Fuel Cells (DC-MFCs) produce electricity (Fig.2.3).
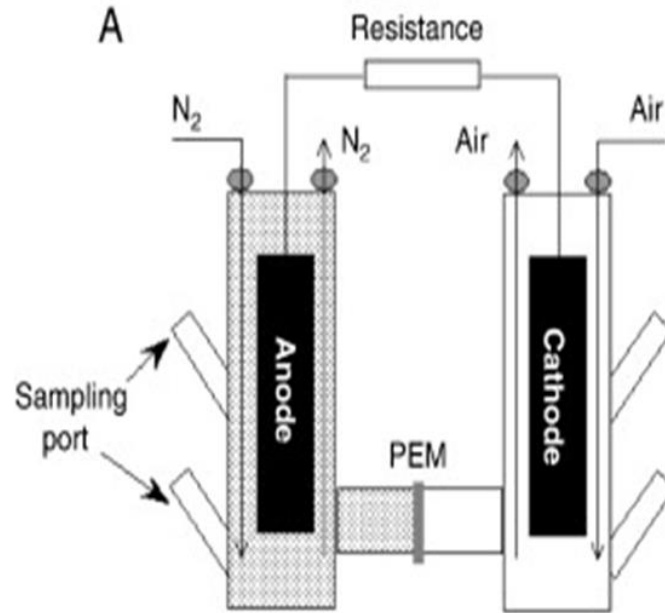
Figure 2.3: Double chambered MFC (DC-MFC)[12]

Bacteria oxidize organic matter in the anode chamber, generating protons and electrons [27].Protons go through the PEM, while electrons travel to the cathode via an external circuit to create an electric current. Water is produced at the cathode when electrons mix with protons and oxygen. Though it has limitations in terms of efficiency, cost, and scalability, this system treats wastewater and generates renewable energy at the same time. Two-compartment MFCs operate in batch mode and are used only in laboratories.

2.4.3 Stacked MFC

Stacked Microbial Fuel Cells (MFCs) improve the power production and efficiency of MFC systems by connecting many units in series or parallel to form a stack (Fig.2.4). Each unit creates electricity through microbial metabolism, and when combined, they dramatically increase overall power output. Voltages increase up while currents remain constant in series designs, which are appropriate for high-voltage purposes; in parallel topologies, currents add up while voltages remain constant, making them perfect for high-current applications [28].

13

This stacking technique, which may also be tailored in hybrid configurations, overcomes the low voltage and power density restrictions of single MFCs by providing increased power output, flexibility, and scalability. However, stacked MFCs have drawbacks such as greater system complexity, higher internal resistance, and maintenance requirements [29].
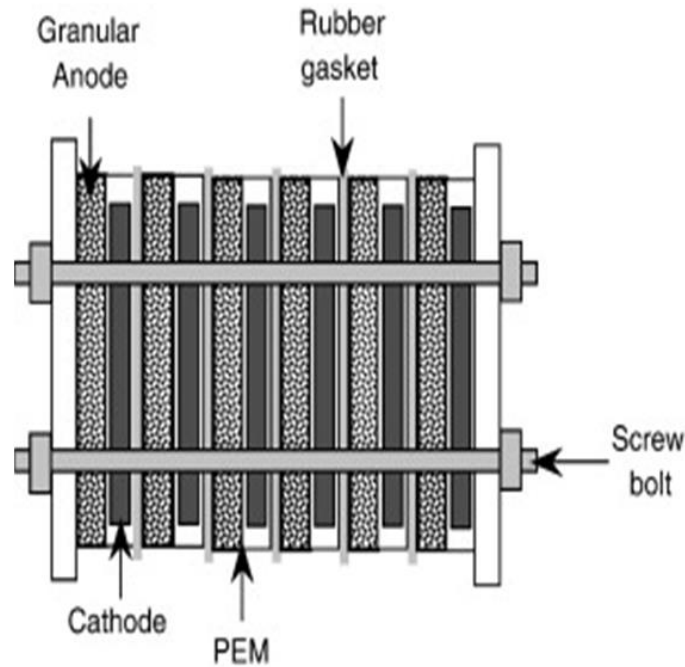
Figure 2.4: Stacked MFC (SMFC)[12]

2.4.4   Up-flow MFC

Up-flow MFCs are cylinder-shaped and made up of a cathode (top) and an anode (bottom) and separated by layers of glass beads and glass wool (Fig 2.5). The feed enters the anode from the bottom, travels up the cathode, and leaves at the top.

The diffusion barrier between the electrodes creates a gradient that allows MFCs to operate properly. Since there is no physical separation in this design, proton transport is unaffected, making it a desirable option for wastewater treatment.

The up flow configuration improves substrate utilization, maximizes microbial activity, and increases overall system efficiency, making it suitable for treating high-

strength wastewater and generating renewable energy in a more compact and effective design [30].
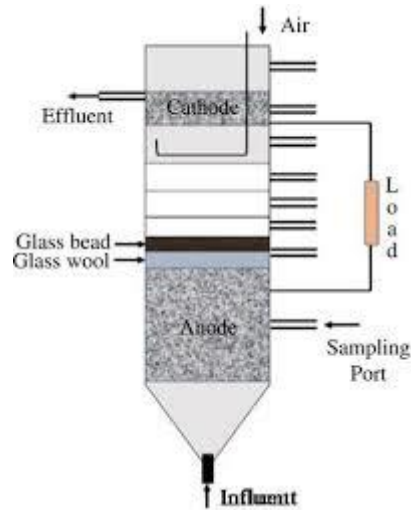
Figure 2.5: Up-flow MFC (UMFC)

2.5   MFC Performance Evaluation

MFCs can be used to generate voltage as well as to treat organic wastes, therefore it is critical to consider both while evaluating them. Table 2 provides a brief discussion of the parameters commonly used to evaluate MFC performance. Internal resistance (Rint), maximum power (Pmax) and open circuit voltage (OCV), can be calculated using the polarization curve (Fig. 2.6).

A polarization curve, which shows voltage as a function of current, is produced by using a potentiostat or various resistors to measure currents (I) at various voltages (Ecell) [7].

In a polarization curve, the relationship between E_{cell} and I is expressed by

$$Ecell~(V) = OCV~(V) - I~(A) \cdot Rint~(\Omega) \qquad (1)$$

R_{int} is the slope of the polarization curve. Power (P) is calculated as

$$P~(W) = I~(A) \cdot Ecell~(V) \qquad (2)$$

15

The polarization curve can thus be used to calculate a power curve. The type of substrate, mediator type, exoelectrogen type, reactor arrangement, anode and cathode material type, and physical conditions like temperature and pH level all affect the MFC's power density [13].

Comparing the performance of different MFC reactors is possible by using the parameters presented in Table 2.
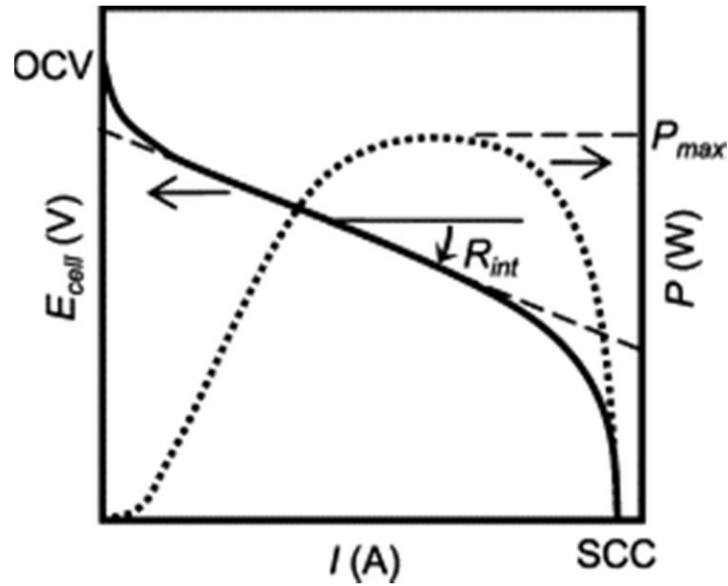
Figure 2.6: Polarization and power curves used for evaluating electrochemical performance of an MFC[14]

Table 2.2: Parameters used for evaluating the MFC performance[31]

Parameter	Unit	Description
Open circuit voltage (OCV)	V	a voltage expressed in terms of current between the anode and cathode
Internal resistance (R_{int})	Ω	derived from the polarization's slope

Coulombic efficiency (CE)	%	The current to total Coulombs contained, measured as (estimated from the total COD value), is known as the Coulomb ratio
Power density (per area)	Wm^{-2}	Anode or cathode areas are used to normalize a power output. When dealing with intricate electrode structures (such as felt or cloth), a projection area is employed
Current density	Am^{-2}	An anode area is used to normalize a generated current
Energy efficiency (EE)	%	The proportion of power generated by MFC to heat energy released during substrate combustion
Treatment efficiency	%	known as COD-removal efficiency, which is calculated by dividing the influent and effluent COD concentrations

2.6   Microbial Electron Transfer Mechanisms

Microbial electron transfer mechanisms are critical for the operation of Microbial Fuel Cells (MFCs) and entail a number of complex processes in which microorganisms move electrons from organic substrates to anode surfaces [32]. These methods can be generically classified as direct and indirect electron transport pathways:

2.6.1   Direct Electron Transfer (DET)

In Direct Electron Transfer, microorganisms transfer electrons directly to the electrode without the need for mediators. This can occur through:

- Outer Membrane Cytochromes are proteins located in the outer membrane of bacteria. These proteins facilitate the transfer of electrons directly from the cell to the anode (Fig.2.7b). Geobacter and Shewanella species possess outer membrane cytochromes that play a key role in DET [33].

- Electrically conductive pili also known as nanowires, extend from the bacterial cells. These nanowires create a physical bridge between the cells and the anode, enabling electron transfer over longer distances. Geobacter sulfurreducens uses conductive pili for efficient DET (Fig.2.7c).

2.6.2 Indirect/ Mediated Electron Transfer (MET)

In Indirect Electron Transfer, microorganisms use soluble or insoluble compounds to shuttle electrons to the anode. This includes:

- Mediator Compounds are external redox active compounds produce by microorganisms that carry electrons [34]. These mediators are reduced by the microorganisms and then diffuse to the anode, where they are oxidized, releasing the electrons (Fig.2.7a). Quinones, phenazines, and flavins can act as electron shuttles.

- Dissolved Redox Compounds are soluble compounds that can diffuse away from the cell. These reduced compounds transfer electrons to the anode directly or through further redox reactions. Iron (Fe^{3+}) and manganese (Mn^{4+}) oxides can be reduced by bacteria and subsequently transfer electrons to the anode.
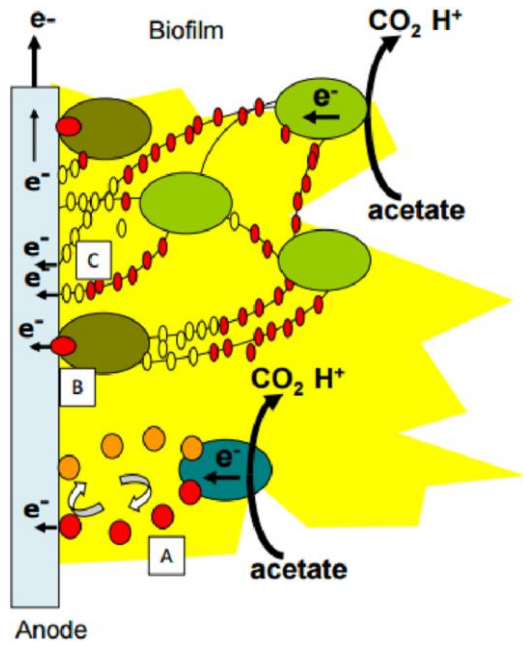
Figure 2.7: Mechanism of electrons transfer in MFCs [1]
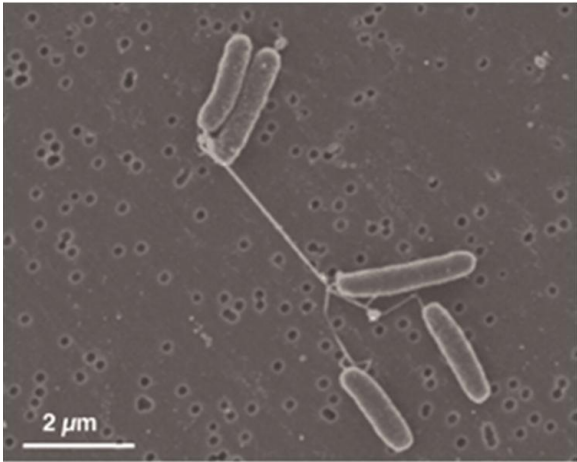
Figure 2.8: Image from Scanning Electron Microscope, Shewanella oneidensis MR-1 produced electrically conductive pilus or nanowires [35]

2.7   Factors Affecting MFC Performance

Microbial fuel cells (MFCs) are devices that use the catalytic activity of microorganisms to transform the chemical energy in organic compounds into electrical energy. MFC performance can be influenced by a variety of elements, which can be

classified as biological, chemical, or physical. Here are several significant parameters that influence MFC performance.

2.7.1 Biological Factors

- Microbial Community

  The efficiency with which bacteria transmit electrons varies significantly. Geobacter and Shewanella species are often used because to their high electrochemical activity[36]. A diversified microbial community can speed up the breakdown of a wide range of substrates. Effective biofilm growth on the anode improves electron transport. The thickness and density of the biofilm also play important effects.

- Substrate Type and Concentration

  Simple substrates (such as glucose) are easier to digest than complex ones (such as lignocellulose). Optimal amounts promote microbial activity, however extremely high concentrations can block substrates or increase internal resistance.

2.7.2 Chemical Factors

- PH The pH of the media influences both microbial activity and electrochemical processes. Most MFCs function well in the neutral pH range (6.5-7.5).

- Conductivity A higher conductivity of the electrolyte minimizes internal resistance and increases power output. Salts or buffers can be used to improve conductivity [37].

- Electron Acceptors The kind and concentration of electron acceptors at the cathode (such as oxygen and ferricyanide) have a major impact on MFC performance. Oxygen is a popular acceptor because of its high redox potential and availability.

2.7.3 Physical Factors

- Electrode Materials

Materials with a large surface area, excellent conductivity, and biocompatibility are chosen.

- Electrode Configuration

The design and positioning of electrodes have an impact on electron transfer efficiency. A shorter distance between electrodes lowers internal resistance.

- Membrane

The type and qualities of the membrane (for example, Nafion) used to separate the anodic and cathodic chambers influence ion transport and substrate crossing, which can have an impact on overall efficiency [36].

- Reactor design

The MFC's architecture, including single-chamber versus double-chamber designs, flow rates, and substrate delivery methods, all have an impact on performance**.**

2.7.4 Environmental Factors

- Temperature

Microbial activity and reaction rates increase with temperature until they reach an ideal point, after which performance can suffer due to enzyme denaturation or microbial mortality.

- Oxygen level

Oxygen exposure to the anode should be limited since it might operate as an alternative electron acceptor, limiting electron flow to the anode and therefore power

generation. By properly controlling these elements, MFC efficiency and power output can be considerably increased**.**

2.8   Different Strategies Enhancing MFC Performance

MFCs are made up of essential components similar to those found in fuel cells. These components consist of a cathode, an anode, an external circuit, and a separator. These components are critical to determining the performance of MFCs.

2.8.1   Anodic Modification

The anode material used in an MFC is critical because it allows electroactive bacteria to develop electroactive biofilms, regulates electron transfer mechanisms, and influences the kinetics of substrate oxidation in the MFC [38]. The power output is determined on the anode material used. The maximum power density limit is a defining feature that has a significant impact on the operation of the MFC. Therefore, anode materials must have outstanding biocompatibility, extraordinary conductivity, chemical stability, minimal internal resistance, high mechanical strength, corrosion resistance, and toughness. Furthermore, the anode must have a large surface area to improve bacterial adherence and maximize the MFC's effectiveness [39]. Previously, numerous anode materials were tested in laboratories to improve the performance and cost viability of MFCs for large-scale deployment. Carbonaceous materials, including graphite fiber brushes and rods, carbon cloth, reticulated vitreous carbon, and carbon felt are commonly used as anodes [39]. Table 3 demonstrates the various anode materials used in recent MFC research. Initially, 2D carbon materials were commonly utilized as anodes in MFC research because they were simple to construct and allowed for precise measurements of biofilm growth [39]. Recent advancements in MFC, as well as breakthroughs in materials and nanotechnology, have increased the use of three-dimensional (3D) anode materials [40].

In addition to upgrading anode materials, electrode pre-treatments (acid, ammonia, and heat) have shown promise in increasing MFC efficiency and power production. For example, employing carbon fabric treated with concentrated ammonia followed by heat

treatment in a muffle furnace and found a higher power density due to increased bacterial attachment to the anode surface [41].

Recently, the usage of unconventional carbonaceous materials has increased, including stainless steel, stainless steel with surface changes, and graphene-based anodes. Chen et al. revealed that composite graphene materials may achieve a much greater power density of 427 mW/m^3 than standard carbon felt anodes [42]. Furthermore, the macroporous graphene sponge used in this study enabled microbe proliferation and diffusion inside the materials, leading to a better electron transport mechanism. Carbon nanofibers [42], single-walled, and multi-walled carbon nanotubes [42] have showed remarkable bacterial adhesion and power production properties. Shen et al. reported a significant increase in power density while using carbon nanofiber-modified graphene compared to naked graphene [43]. Exploring various advanced materials for surface modification and elemental dosing could be a valuable approach to boost anode efficiency and enhance overall performance.

Table 2.3: Summarized various anodic materials [44]

Anode Materials	Methods of Fabrication	Advantages
Natural biomass derived	Carbonization	3D permeable architecture, eco-friendliness, and little pollution
Metal based	Co-precipitation method, Hydrothermal method, Electrodeposition method	Normalize the surface characteristics
CNTs based	Layer by layer assembly, Liquid-liquid interface transfer process	Excellent mechanical properties, Favorable catalytic activity

23

Graphene based	Solution casting process, Layer by layer assembly method	Features high active surface area and outstanding electrical properties
Conducting polymer based	Electrodeposition method, Electrochemical polymerization process	Suitable synthesis, moderately high cost, eco friendly

2.8.2   Cathodic Modification

The two most popular cathode configurations are air-cathode and aqueous phase cathodes. An air-cathode MFC allows for direct exposure of the reaction region to air, which eliminates aeration costs and increases MFC power density [44]. Typically, an air-cathode MFC consists of a hydrophobic diffusion layer that is exposed to air, a catalyst layer/binder that is in contact with water, and a conductive supporting material that may also serve as a diffusion layer. In contrast, an aqueous phase cathode employs a catholyte in a separate reaction chamber and is comprised of a conductive supporting layer as well as a catalyst/binder layer. The cathode material and design present considerable hurdles in an MFC, as slow cathode dynamics frequently impede MFC performance. Carbon-based materials are often utilized as cathode bases because they are abundant, inexpensive, and versatile[44]. These materials listed above also function as cathodes. One popular cathode design uses a carbon basis (paper/cloth) coated with a platinum (Pt) catalyst on one side, often with the help of a binder solution. Researchers developed a more practical and cost-effective way for creating air cathodes that uses stainless steel as a supporting material rather than carbon paper and cloth [44].

Anode materials can also function as cathodes, with the sole difference being the need for a catalyst layer to improve the oxidation-reduction reaction (ORR). For example, Pt or ferricyanide catalysts are commonly used in dissolved oxygen or gas diffusion cathodes [45]. Additionally, catalysts manufactured from non-precious metals, such as

iron-based compounds [44] and activated carbon, have been tested in laboratories. When adding catalyst to the cathode, a binder/polymer is required [45]. In the world of MFC, binders are perfluorosulfonic acid (Nafion) and polytetrafluoroethylene (PTFE) [44]. A comparison was conducted between PTFE and Nafion to assess their ability to achieve high power density in a single chamber MFC [46]. The Nafion binder outperformed PTFE, increasing power density by more than 20%. The PTFE binder had a lower power density because it formed a loose and thin biofilm. Nevertheless, the substantial power density achieved with Nafion [44] cannot be economically justified on a broad scale because to its excessive cost as compared to PTFE. So, choice of efficient cathode material is crucial for better performance of MFCs.

2.8.3   Membrane Modification

Membrane separators offer various advantages, including the prevention of oxygen transport and substrate crossing between the anode and cathode. However, integrating a membrane greatly raises the costs associated with MFC design, limiting its potential for widespread commercial use [47]. As a result, proper membrane selection is critical in the design of MFCs, as they account for a major amount of the total cost. Furthermore, membranes can lead to higher internal resistance and occasionally allow oxygen penetration, resulting in a drop in MFC efficiency. Membrane biofouling is a key challenge, undermining the feasibility of deploying membrane MFCs in real-world applications [48].

The use of porous and low resistance membranes, such as microfiltration membranes, can reduce both coulombic efficiency and power density. This is because these membranes enable substrate crossover and oxygen permeability [49]. Understanding oxygen migration from the cathode to the anode is critical because it can have a substantial impact on MFC performance and result in voltage loss due to changes in redox potential induced by aerobic microorganisms consuming substrates rather than anaerobic electrogens. Furthermore, oxygen, a more preferred electron acceptor, competes with the anode for electrons [50], reducing the overall efficiency of the MFC. So, selecting a specific sort of membrane is critical.

2.9   Proposed Anodic Materials

2.9.1   MXene (Ti$_3$C$_2$T$_x$)

In recent years, a vast new family of two-dimensional transition carbonitrides, metal carbides and nitrides known as MXene has gained a lot of attention because of its numerous unique physical and chemical features [51]. As they have much in common with the wide diversity of their surface terminations and elemental compositions. MXenes are easily incorporated into composites with oxides, polymers, and carbon nanotubes, offering a useful way to alter their characteristics for a range of uses (Fig. 10.). As it is well known, MXene and MXene-based composites have become popular as electrode materials in the energy storage industry, and they have also demonstrated tremendous promise in environmental applications like electro/photocatalytic water splitting, photocatalytic carbon dioxide reduction, and water purification [52], and reducibility, high conductivity, and biocompatibility make them ideal for various applications.
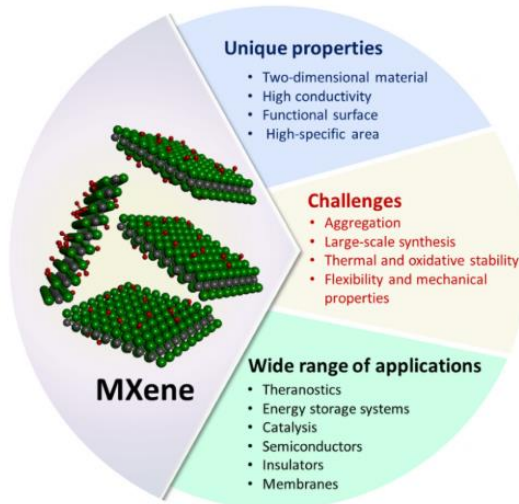
Figure 2.9: MXene and its properties [51]

"MXene" is a rapidly developing material. MXenes are primarily synthesized by etching the A layers from MAX phases, which are ternary nitrides or carbides with the general chemical formula $M_{n+1}AX_n$, where M represents an early transition metal, A is a group IIIA or IVA element, X is C and/or N, and n = 1, 2, or 3. MAX phases have layered hexagonal structures in which the $M_{n+1}X_n$ units and the A layers alternately stack. Because

the M-X bonds are substantially stronger than the M-A bonds[53], the A layers can be selectively etched without damaging the M-X bonds, yielding weakly bonded $M_{n+1}AX_n$ layers that can be easily separated using sonication. The generated 2D materials are known as MXenes because they lose A layers from the parent MAX phase and have a 2D structure like graphene.

It should be noted that throughout the etching process, the surfaces of the $M_{n+1}AX_n$ units are invariably coated with functional groups such as oxygen (O), hydroxyl (-OH), and/or fluorine (-F). So, the chemical formula for MXene is $M_{n+1}AX_n$, where T_x represents the surface functional groups.
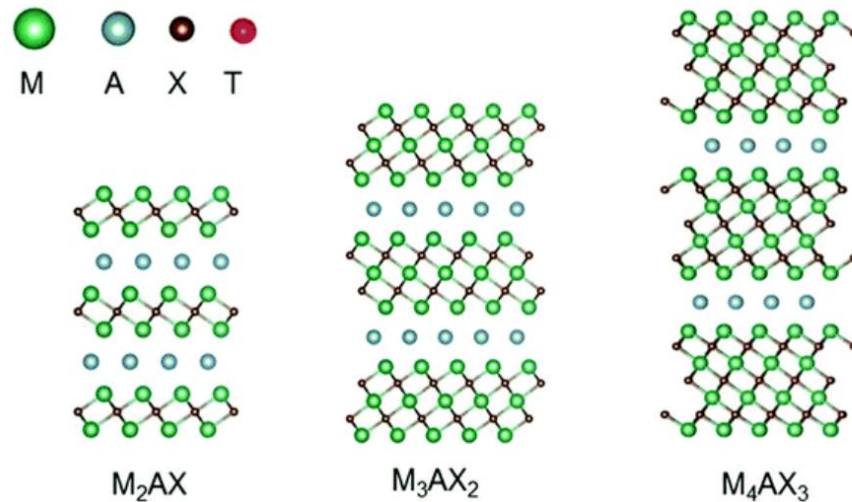
Figure 2.10: MXene ($M_{n+1}AX_n$) structure [53]

Wang et al. found that after one day of inoculation with a bacterial combination, a two-dimensional Ti_3C_2 MXene anode successfully powered the MFC. The output voltage was 640 ± 8 mV with an external resistance of 1000 Ω and a maximum power density of 3.74 W/m^{-2}, much greater than the carbon cloth (CC) control (550 ± 8 mV and 2.05 W/m^{-2}).

Multilayer structure, high surface area, and better conductivity of Ti_3C_2 MXene help boost MFC output performance and provide more active sites for biological redox processes [54].

2.9.2 Polypyrrole (PPy)

Polypyrrole is a unique and flexible organic polymer that belongs to the conducting polymer class, also known as "synthetic metals." Polypyrrole's chemical structure consists of repeated pyrrole (C_4H_4NH) units (Fig 2.11). Each pyrrole ring is joined head-to-tail at locations 2 and 5, forming a conjugated structure that allows polypyrrole to have its particular electrical conductivity [10].
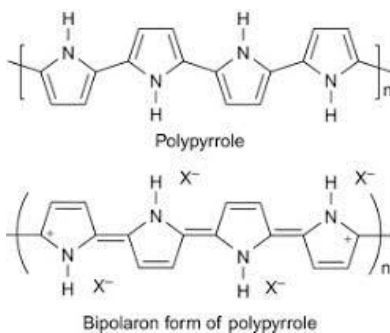
Figure 2.11: Structure of polypyrrole

Polypyrrole (PPy) has garnered special attention among conducting polymers because of its high electrical conductivity, excellent redox characteristics, and inexpensive production costs. PPy-based materials have good redox reversibility and high electrical conductivity [55]. Additionally, they have exceptional thermal stability. Polypyrrole can also be employed in composite materials including carbon nanostructures. Pyrrole can be easily polymerized chemically or electrochemically to produce PPy [56]. Pyrrole polymerization occurs in the presence of a variety of oxidizing agents, including iron (III) sulfonates, iron (III) chloride ammonium persulphate (APS), potassium dichromate (PDC), iron (III) complexes and H_2O_2.

Zou et al. found that nanostructured electrically conductive polymer polypyrrole dramatically improved electron collection efficiency from photosynthetic biofilms in photosynthetic microbial fuel cells (PMFCs). Cyclic voltammetry and electrochemical impedance spectroscopy studies revealed that nanostructured anode materials outperformed conventional anodes due to considerable improvements in electrochemical properties, such as higher redox current and lower interface electron transfer resistance. At

a loading density of 3 mg/cm^2, coating an anode with fibrillar polypyrrole resulted in a 450% increase in power density [57].

2.10   Novelty (PPy/MXene) Composite

My proposed anodic material is composite of PPy/MXene. That is not confirmed by literature. MXene and polypyrrole (PPy) have complementary properties, making their composite an ideal choice for anodic materials in microbial fuel cells (MFCs). MXene has outstanding electrical conductivity, mechanical resilience, and high surface area due to its layered structure, which allows for efficient electron transfer and provides numerous active sites for microbial adhesion. Polypyrrole, as a conducting polymer, increases overall conductivity while also contributing increased surface area due to its porous structure. The biocompatibility of both materials contributes to the composite's ability to sustain microbial growth and activity, which is critical for MFC functioning. Additionally, MXene provides chemical stability across various environments, while the inclusion of PPy, known for its facile synthesis and doping capabilities, further improves the composite's properties. Enhanced electrocatalytic activity and improved mechanical strength make the PPy/MXene composite a better choice for enhancing performance and efficiency in MFC applications.

CHAPTER 3: MATERIALS AND METHODS

3.1 MXene (Ti_3AlC_2)

$Ti_3C_2T_x$-MXene nanosheets (MXene) were obtained from MAX by etching Al layer with the help of HF. Firstly, oil bath was prepared for the purpose of uniform heating and maintained its temperature to 50℃ then added 20ml of HF in Teflon cup and placed it within oil bath. Subsequently, 1g of MAX phase was added bit by bit into HF. And stirred it at 600rpm for 24 hours.

Then diluted MXene with DI water and centrifuged it at 4500rpm for 6-7 times until its PH was maintained to ≥ 6. Then placed it in drying oven at 65℃ for 24 hours. Next step is separation of MXene sheets by adding intercalating agent as 45ml of DMSO was added into above etched MXene and stirred it on hotplate for 20 hours at room temperature.

Then again centrifuged it 5-6 times for washing purpose until its PH was maintained to neutral. After this MXene solution was placed in probe sonicator for 3hrs 45min. In the end the solution was centrifuged one time at 3000rpm for sample collection. Finally, MXene nanosheets were obtained after drying it for 24 hrs in drying oven.

3.2 PPy/MXene Composite

Firstly, 1M HCL was taken i.e. 23ml DI water and 2ml HCl was mixed to make 25ml in total and then 0.25g of MXene was added into it. The above solution was ultrasonicated for 1h. After 1h, 0.15ml of pyrrole was added in the above solution and vigorously stirred for 2h. Then in an ice bath temperature was maintained to 0 - 4℃. 400mg of APS solution was made by dissolving it into 10ml of DI water then it was added dropwise with the help of micropipette in above solution while placing it in ice bath and vigorously stirred it in ice bath for further 7h.

In the end it was centrifuged at 3000rpm for 3 times and then dried it in drying oven for 15 h. Finally, MXene- polypyrrole composite was obtained by in-situ polymerization process.
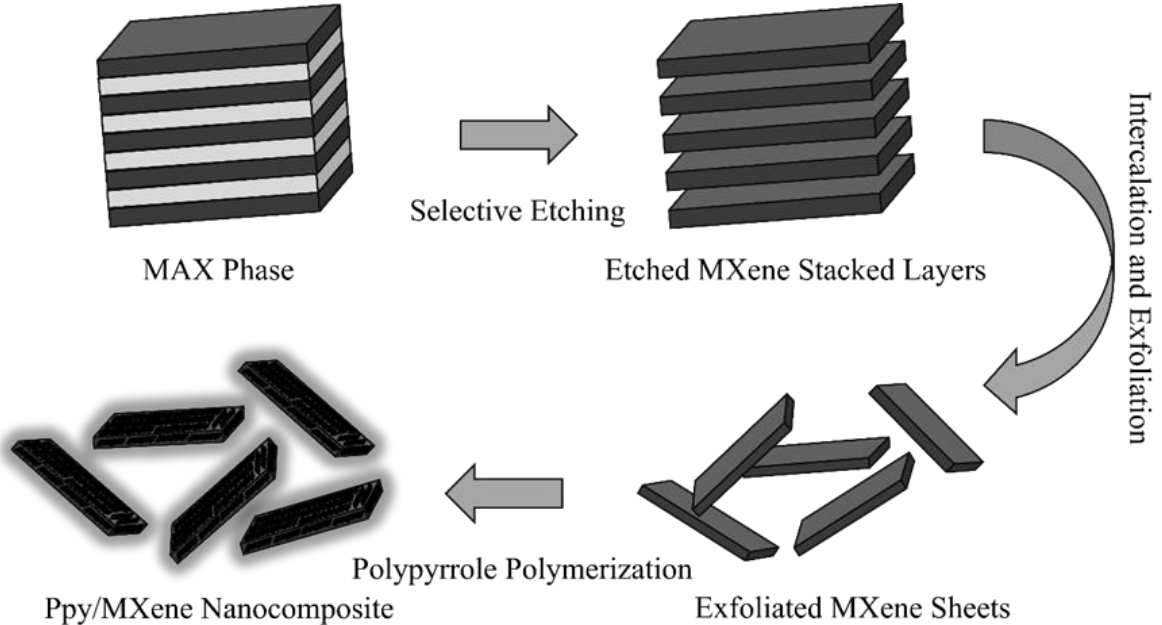
Figure 3.1: Synthesis process of Ti$_3$C$_2$ MXene and PPy/MXene Composite

3.3   Preparation of Anode

The anodic electrode was prepared using following steps:

3.3.1   Hydrophilic Treatment of Anode

The Graphite felt (GF) was cut into 3.3×3.3 cm^2 pieces. It was immersed in acetone solution for 24 hours to remove surface oil contaminants, and then it was cleaned with ethanol under ultrasound for 30 minutes. Subsequently, it was treated with 10% H$_2$O$_2$ and 10% HCl in a 90 °C water bath for 3 hours.

After thorough rinsing with deionized water and drying at 60°C overnight, hydrophilic graphite felt was obtained.

3.3.2 Slurry Preparation

The initial step involved the formation of a slurry for coating on anode. Slurry of MXene and PPy/MXene composite was separately prepared. 88mg of MXene powder and PPy/MXene was mixed with 220µl of Nafion 117 solution that acts as a binder, followed by 3.3 ml of ethanol and 550µl of DI water. These two samples were sonicated separately in ultrasonic bath for 3-4 hours until uniform suspension was obtained.

3.3.3 Slurry Coating on Anode

To ensure even distribution of the coating, a slurry was applied to the GF using the dip and dry process. The coated GF was then vacuum dried in an oven set at 70°C for a full night.

To calculate the mass loading, the weight of the graphite felt was measured both before and after the coating procedure. Table 3.1 mentions mass loading below.

Table 3.1: Mass Loading

Graphite Felt	Initial Weight	Final Weight	Mass Loading
Bare GF	870.00 mg	870.00 mg	0%
MXene (Ti_3AlC_2) Coated GF	874.52 mg	925.12 mg	92%
MXene /PPy Coated GF	871.61 mg	924.41 mg	96 %

3.4 Membrane Pretreatment

Three separate steps of pre-treatment were applied to the Nafion 117 membrane. The first step involved heating the membrane for an hour at 80 degrees Celsius in distilled water.

It was then immersed for two hours at the same temperature in a 3% hydrogen peroxide solution. Lastly, it was treated for two hours at 80°C with a 0.5 M sulfuric acid solution.

After that, the PEM was placed in deionized water to be stored before use.

3.5   MFCs Setup

The experiments were conducted using the dual chamber MFC setup, as Fig. 2.3 illustrates. Every chamber in the reactor has a total volume of 100 milliliters.

3.5.1   MFC Construction

Every piece of the MFC setup was built manually. A laser cutting equipment was used to cut a sheet of Plexiglass that was obtained from the market into multiple sizes. Once assembled, the parts were sealed against leaks by applying adhesive to create two separate compartments.

A rubber gasket was then attached to one side of each chamber. To make the holes required for sample collection, nitrogen purging in the anodic chamber, and air purging in the cathodic chamber, drilling was done on the top plate. After the membrane is positioned between the chambers, nuts and screws are used to firmly secure the chambers together.

3.5.2   MFC Arrangement

The anode was placed inside the anodic chamber, which was already filled with anolyte. The anodic chamber was fully sealed with silicon sealant to keep any air from getting inside.

Similar to this, catholyte was poured into the cathode and it was positioned inside the cathodic chamber. Cathode is simply a polytetrafluoroethylene (PTFE) coated carbon cloth (CC) of area 3.3cm x 3.3cm.

Within the cathode, a pipe was placed for air purging. For the anolyte to disperse uniformly, the complete MFC apparatus was placed on a magnetic stirring plate to

guarantee constant swirling. To guarantee the ideal temperature for bacteria, an automatic heating rod set at 34°C was positioned close by.

3.5.3   Microbial Sludge

The original inoculum, or anaerobic reactor sludge, was taken from NUST University in Islamabad, Pakistan's membrane bioreactor wastewater treatment facility.

The foreign particles were removed from the sludge by sifting it and constantly shaking it at 180 rpm. As a result, the final microbial inoculum was produced in a homogenous liquid phase.

The sludge was replenished and added to new growth media after pretreatment. To make it easier to add new media and remove old media, the flask was equipped with ports.

3.5.4   Anolyte

The substances shown in table 3.2, along with their corresponding amounts, make up the anodic media. To create an oxygen-free atmosphere, 100% nitrogen gas was used to purge the medium.

In addition, to avoid any bacterial development or consumption, the medium is made fresh every time. The 70% depleted media was then separated by decantation and replaced with a fresh growth medium after each drop in voltage values. Each cycle is followed by a repetition of this exercise.

Table 3.2: The concentration of minerals in a nutrient solution

Sr no.	Salt name	Chemical Formula	Concentration (g/L)
01.	Manganese Sulphate	$MnSO_4.H_2O$	0.50
02.	Sodium Chloride	$NaCl$	1.00

03.	Iron sulphate	$FeSO_4.7H_2O$	0.10
04.	Calcium Chloride	$CaCl_2.2H_2O$	0.10
05.	Zinc Sulphate	$ZnSO_4.7H_2O$	0.18
06.	Copper Sulphate	$CuSO4.5H_2O$	0.01
07.	Boric Acid	H_3BO_3	0.01
08.	Ammonium Chloride	NH_4Cl	1.00
09.	Sodium Citrate	$C_6H_5Na_3O_7$	0.3
10.	L-ascorbic Acid	$C_6H_8O_6$	0.1
11.	Cobalt Chloride	$CoCl_2$	0.1
12.	Nickel Nitrate	$Ni(NO_3)_2$	0.03
13.	Magnesium Chloride	$Mg Cl_2$	0.06

3.5.5   Catholyte

A 0.5 M solution of potassium phosphate buffer with a pH of 7 served as catholyte. For effective reduction, oxygen, or air, was continuously supplied to the cathode chamber via an air pump.

Every time the PBS solution evaporates and dries out, it is entirely restored on the cathodic side.

3.6   MFC Operation

Three different MFCs comprised of anodes as bare GF, MXene coated GF and PPy/MXene coated GF were placed on specific stable area and were connected to a common data logger as shown in Fig 3.2.

Real time data was obtained from Picolog software on personal computer.
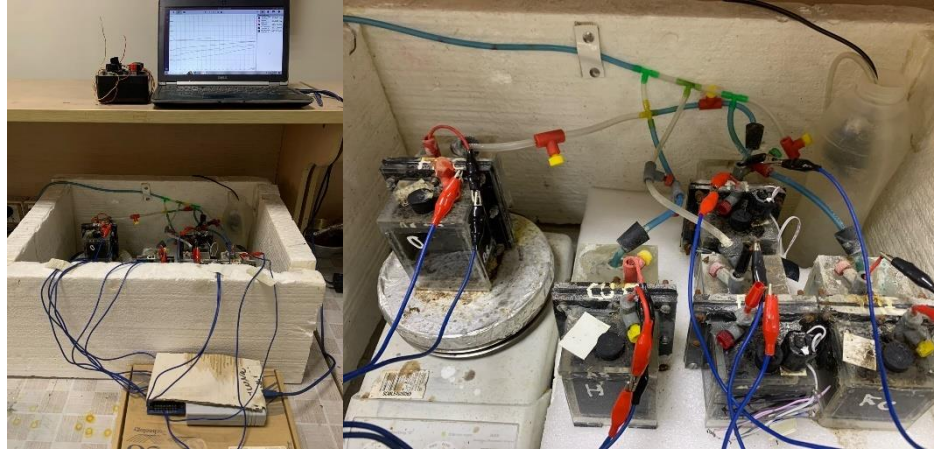
Figure 3.2: Our designed MFCs

To get open circuit voltage (OCV), initially solution comprises 1000 COD was filled in anodic chamber of all three cells and cycle was run for 7-8 days until it was completed. Then in a similar fashion 500 COD cycle was run and finally 500 COD with 1000Ω resistor cycle was obtained. Polarization curves were used to obtain the maximum power density by varying the external resistance from 10 to 10,000 Ω at different voltage values. Current density and power density was calculated by dividing obtained current and power with electrode cross-sectional area as:

$$I = V/R \qquad \ldots\ldots\ldots\ldots (1)$$

$$\text{Current density} = I/A \qquad \ldots\ldots\ldots\ldots (2)$$

$$\text{Power} = IV \qquad \ldots\ldots\ldots\ldots (3)$$

$$\text{Power density} = P/A \qquad \ldots\ldots\ldots\ldots (4)$$

Where I is current, V is voltage, R is resistance, A is cross-sectional area and P is power. A graph was plotted b/w Power density (mW/m^2) and current density (mA/m^2). Finally coulombic efficiency is calculated to get the idea of effectiveness of the microbial community and the electrode materials in converting organic matter into electricity.

$$CE = \frac{8 \text{ x } I \text{ x } \Delta t}{\Delta COD \text{ x } V \text{ x } 96,485} \qquad \ldots\ldots\ldots\ldots (5)$$

where Δt is the batch time duration, I is the average current, V is the volume of wastewater treated, ΔCOD is the difference of COD value between influent and effluent of anode chamber, based on 32 being the molecular weight of oxygen and 4 electrons in 1 mol of oxygen, the constant is 8.

CHAPTER 4: CHARACTERIZATION

4.1   Instruments

X-ray diffraction (XRD), Scanning electron microscopy (SEM) and Fourier transform infrared spectroscopy (FTIR) were used to evaluate the samples. To get both qualitative and quantitative results, other techniques such chemical oxygen demand (COD), electrochemical impedance spectroscopy (EIS), cyclic voltammetry (CV) were used. Every characterization process is covered in detail in the section that follows.

4.2   Scanning Electron Microscopy (SEM)

4.2.1   Working Principle

Using this method, a narrow electron beam is precisely focused onto an object's surface. Particles like photons or electrons are consequently forced off the material's surface. The released electrons are then guided into the detector for additional examination. The cathode ray tubes (CRT) brightness varies as a result of the signal produced by the detector. The material's image is created by plotting a corresponding point on the cathode ray tube (CRT) at each location where the beams interact [58].

X-rays, backscattered electrons (BSE), and secondary electrons (SE) are released when surfaces contact with electrons [59]. Secondary electrons are used in scanning electron microscopy (SEM) as the main means of detection. These electrons are released in close proximity to the sample's surface. As a result, a clear and distinct image of the specimen is obtained.

This method can detect minuscule details with sizes smaller than one nanometer. Furthermore, when input electrons interact with a target material, backscattered electrons are released, a phenomenon known as elastic scattering takes place. Compared to primary electrons, secondary electrons are found at shallower depths. In contrast, the resolution of the specified entity is a little bit lower. There are specific features that are released when an electron in the inner shell breaks free of its orbit [60].

Figure 4.1: SEM (JEOL) present at SCME, NUST.

4.2.2   Important Features

The basic sample preparation procedures of scanning electron microscopy (SEM) make it a popular tool for studying several features of a sample, such as its morphology, chemistry, crystallography, and plane orientation. The variable magnification range of the scanning electron microscope (SEM) is 10 to 500,000 times. Any instrument can be used to examine the materials' morphology, however a FESEM will yield higher resolution.

An Energy Dispersive X-ray Spectroscopy (EDS) detector coupled to a Field Emission Scanning Electron Microscope (FESEM) can be used to determine the elemental composition [61].

4.2.3   Sample Preparation

The sample was preheated or dried in a drying oven set to 60°C for 3 hours. This step was performed to remove any moisture that may have been present or trapped within the layers of the material. The dried samples were then immediately transferred to the stub or sample holder of the SEM apparatus for analysis.

4.3   Xray Diffraction (XRD)

4.3.1   Working Principle

The goal of this procedure is to determine the material's crystal structure. The aforementioned method is non-destructive and aids in the acquisition of Bragg's reflection fingerprints from crystalline materials [62]. The composition consists of three basic components. The experimental setup includes a cathode tube, a sample container, and a detector. X-rays are generated via the process of thermionic emission, which involves heating a filament element to high temperatures, triggering the emission of electrons [63].

Figure 4.2: XRD (BRUKER) present at SCME, NUST.

These electrons are then propelled towards a target material, colliding with its electrons and producing X-rays. Crystal structure is defined by the presence of discrete layers and planes.

An X-ray with a wavelength similar to the planes in question is reflected at an angle of incidence equal to its angle of reflection. "Diffraction" happens and can be accurately explained by Bragg's Law [63].

$$2dsin\theta = n\lambda \qquad ………2$$

When Bragg's law is met, it shows the presence of constructive interference, which causes the detector to detect "Bragg's reflections". The positioning of these reflections reveals the inter-layer spacing, whereas ray diffraction analysis tells us about the sample's phase, crystallinity, and purity [64]. Using this technology, it is also feasible to determine

lattice misfit, dislocations, and unit cell size. X-ray diffraction investigations were carried out at the National University of Sciences and Technology's School of Chemical and Materials Engineering (SCME-NUST).

4.3.2   Sample Preparation

The samples were undergoing an initial preheating or drying process in a drying oven set to 60°C for 3 hours. This step was performed to remove any moisture that may have been present or trapped within the layers of the material. The dried samples were then immediately transferred to the stub or sample holder of the X-ray diffraction (XRD) apparatus for analysis.

4.4   Fourier Transform Infra-Red (FT-IR) Spectroscopy

4.4.1   Working Principle

A light source generates infrared (IR) radiation, which is then focused on the sample. The sample selectively absorbs specific portions of the passing light while reflecting the remainder. The leftover light is delivered, containing the chemical data, and then collected by a detector to produce an electronic signal [65]. The Fourier transform infrared spectrometer relies heavily on the Michelson interferometer. Figure 4.3 depicts how the source's infrared beam goes through the interferometer and is directed towards a beam splitter for measurement. The beam is then separated and directed towards a fixed mirror and a mirror in motion. The beam is then combined and targeted toward the sample material. The spectral information for all wavelengths is obtained concurrently. The mobile mirror varies the lengths of the optical pathways, causing light interference between the two divided beams.

There won't be a path difference if the moving mirror is positioned the same distance from the beam splitter as the fixed mirror. This is because the optical pathways of both split beams will be similar. When the moving mirror is shifted away from the beam-splitter, an optical path difference (δ) is created. Alternating destructive and constructive

interference is produced by the two split beams [66], with a steady fluctuation in the δ value.

Constructive interference occurs when;

$$\delta = n\lambda$$

Destructive interference occurs when;

$$\delta = (1 / 2 + n) \lambda$$

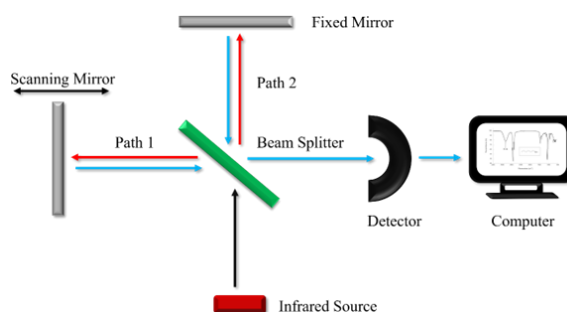A change in the position of the moving mirror results in a change of δ value.

Figure 4.3: FTIR (Perkin Spectrum 100) present at SCME, NUST.

4.4.2   Important Features

Infrared spectroscopy studies the interaction between infrared radiation and material. A form of electromagnetic radiation having a wavelength greater than visible

light is called infrared radiation. The most prevalent approach for vibrational spectroscopy is FTIR, which is used to identify functional groups and chemical bonds [67]. Fourier transform infrared spectroscopy (FTIR) is a technique that captures an infrared spectrum over a wide range of wavenumbers.

The dispersive method differs from this approach in that it collects signals independently at each wavenumber to generate a spectrum. FTIR has essentially replaced the dispersive approach because of its substantially higher signal-to-noise ratio. An FTIR spectrum can be compared to a chemical fingerprint [68].

It can identify and authenticate known and unknown samples, as well as evaluate and describe new materials. Especially useful in the chemical and industrial industries, as well as research and development.

4.4.3   Sample Preparation

The materials were first preheated or dried in a drying oven at 60°C for 3 hours. This procedure was taken to remove any moisture that may have been present or trapped between the layers of the material. The dried samples were then one by one added to KBr of required amount to make pallet. KBr pallet technique was used here. The palette is then put into stub or sample holder of FTIR to make analysis.

4.5   Brunauer-Emmett-Teller (BET)analysis

The Brunauer–Emmett–Teller (BET) specific surface areas were measured by the nitrogen adsorption-desorption method using micromeritics Gemini VII (surface area and porosity), USA (Fig 4.4). It is based on the 1938 theory by Edward Teller, Paul Hugh Emmett, and Stephen Brunauer, which describes the physical adsorption of gas molecules on a solid surface.

The BET method measures the amount of gas (usually nitrogen) that is adsorbed at various pressures and constant temperatures on a material's surface. To create an adsorption isotherm, the data is utilized.

According to the BET theory, gas molecules first form a monolayer on the surface before developing into multilayers. The specific surface area is determined using the volume of gas absorbed at the point where the monolayer coverage is complete.

Figure 4.4: BET micromeritics Gemini VII, USA present at SCME, NUST.

4.5.1   Sample Preparation

To get rid of any pollutants or moisture that have been absorbed, the sample is usually degassed.

4.5.2   Adsorption Measurement

The adsorbate gas, such as nitrogen, is added after the sample has been chilled, usually with liquid nitrogen. It measures how much gas is absorbed at different pressures.

4.5.3   Data Analysis

The BET equation is used to visualize the adsorption data. The linear segment of the diagram is utilized to compute V m and C.

4.5.4   Surface Area Calculation

The following formula is used to determine the specific surface area (S):

$$S = V_m N_A \sigma / m$$

N_A is Avogadro's number. The adsorbate molecule's cross-sectional area is represented by σ. The mass of the sample is given by m.

4.6   Contact Angle Analysis

The optical contact angle measuring system (OCA 15 Plus, Dataphysics, Germany) was employed to measure the contact angle of electrode coated materials (Fig 4.5). The measurement of a solid surface's wettability by a liquid is known as contact angle analysis, and it focuses upon adhesion, surface energy, and hydrophobicity/hydrophilicity. The angle created at the interface where the liquid and solid surfaces meet is known as the contact angle. To guarantee precise and accurate results, the equipment utilized for this measurement usually consists of the following steps.

Figure 4.5: (OCA 15 Plus, Data physics, Germany) present at SCME, NUST.

4.6.1   Sample Preparation

To ensure the measurement is accurate, clean the solid electrode surface to get rid of any impurities. Then coat it with material of which we are going to perform contact angle analysis.

4.6.2 Droplet Dispensing

Apply a droplet of liquid to the solid electrode surface using the precision syringe. For repeatability to be guaranteed, the droplet's volume must remain constant.

4.6.3 Picture Capture

As the droplet rests on the surface, pictures are taken of it by the high-resolution camera. Clear visibility of the droplet's profile is ensured by appropriate lighting.

4.6.4 Angle measurement:

After analyzing the droplet images, the software finds the tangent at the point where the liquid, solid, and air meet in order to calculate the contact angle.

4.6.5 Data Analysis

Surface energy estimates, advancing and retreating angles, and hysteresis are just a few of the extra data that the software may offer.

4.7 Cyclic Voltammetry (CV)

Cyclic voltammetry (CV) is a popular electrochemical technique that includes sweeping the potential to obtain information about the electrochemical process. The CV can be used to identify the redox process of electrode materials, the reactants involved, and the reaction kinetics of heterogeneous electron transfer reactions that occur in an electrochemical.

4.7.1 Working Principle

To perform cyclic voltammetry, an electrochemical cell is built by adding an electrolyte solution and three electrodes. The Gamry potentiostat sweeps the potential between the reference and working electrodes linearly until it reaches a predefined limit, at which point it reverses direction. The CV concept is based on rapid voltage scanning, which involves reversing the voltage scan direction [69].By applying a voltage to the working electrode in both forward and backward orientations, the CV method enables the

measurement of the resultant current as a single or several cycles. The determination of half-peak potentials, anodic and cathodic peak currents, and both can be accomplished using the CV approach.
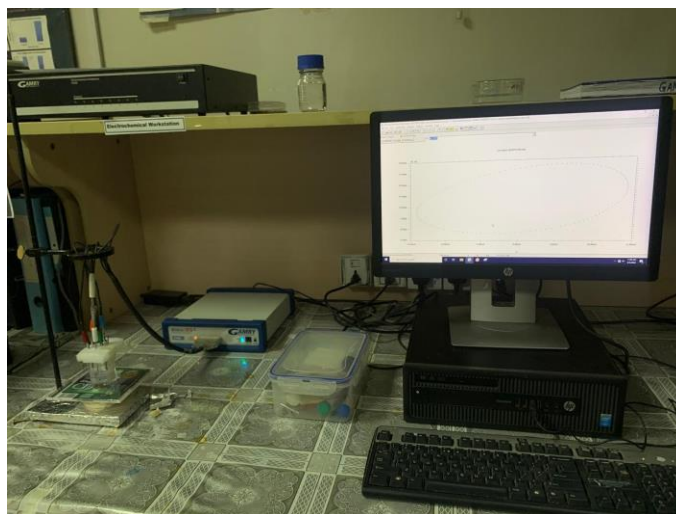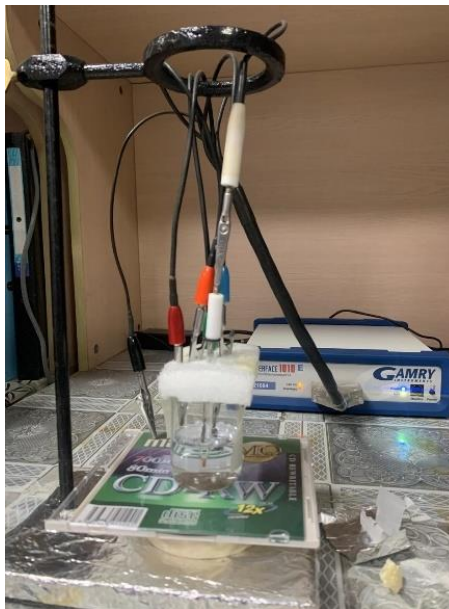

Figure 4.6: Gamry potentiostat present at SCME, NUST

A three-electrode configuration is required, consisting of a reference electrode (RE), a counter electrode (CE), and working electrodes (WE) (Fig. 4.6). To stabilize the solution potential, the reference electrode measures and controls the voltage across the working electrodes [70].

The counter electrode permits current to travel, balancing it through the active electrode According to the Randles-Sevcik equation, the peak current I_p in CV is proportional to both the concentration, C, and the scan rate, v as shown in equation.

$$i_p = 269,000AC(n^3Dv)^{1/2}$$

4.7.2 Applications of CV

Cyclic Voltammetry is a versatile tool for scientific innovation and study since it involves electron transport, which can be tracked using this technique. Its applications include characterization, synthesis, mechanism, and analysis [71]. In all applications, the approach is compatible with a wide range of substances, including organic, inorganic, polymer, films, and semiconductors. It is used as an analytical technique in a variety of fields, including chemistry.

4.8 Electrochemical Impedance Spectroscopy (EIS)

The method used to investigate the kinetics and operations of diverse electrochemical systems is called electrochemical impedance spectroscopy, or EIS. In electrochemical stimulation (EIS), an electrochemical system in equilibrium or steady state is perturbed by applying a sinusoidal signal (voltage or current) at different frequencies. The response of the system is then measured and expressed as voltage or current [72].

4.8.1 Working Principle

The concentration of electroactive species, charge and mass transfers from the bulk solution to the electrode surface, and electrolyte resistance are examples of matter (redox species) electrode interactions in a typical electrochemical cell [73]. As seen in Fig 4.7, an electrical circuit made up of resistances, capacitors, or constant phase components coupled in series or parallel to form an equivalent circuit describes each of these attributes.

EIS can investigate inherent properties of materials or specific procedures that might have an impact on an electrochemical system's capacitance, resistance, or conductance. Since resistance in DC circuits directly obeys Ohm's Law, impedance differs

from resistance. Utilizing a mild signal stimulation, the impedance response is measured [74]. The electrochemical cell response is pseudo-linear, resulting in a phase shift, but the current response to a sinusoidal potential is sinusoid at the applied frequency. Thus, the excitation signal is displayed as a function of time, as indicated in Equation (2)

$$E_t = E_0 sin(\omega t) \tag{2}$$

E_t represents the potential at time t, E_0 is the signal's amplitude, and ω is the radial frequency.

In a linear system, the signal's phase (Φ) and amplitude diverge from I0 as in Equation (3).

$$I_t = I_0 \sin(\omega t + \Phi) \tag{3}$$

Thus, Equation (4) can be used to get the total system impedance

$$Z = E/I = Z_0 \exp(i\Phi) = Z_0(cos\Phi + isin\Phi) \tag{4}$$
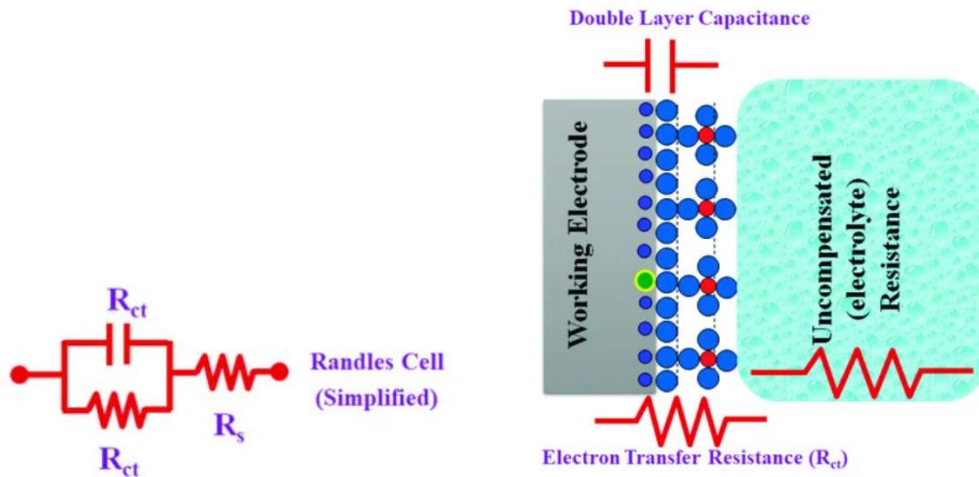
Figure 4.7: Randles Circuit and basic mechanism on electrodes

4.8.2 Applications of EIS

In battery research, EIS is used to measure performance, identify deterioration mechanisms, and optimize materials. In fuel cells, it assesses catalyst and membrane

performance. EIS is essential in corrosion research for determining corrosion rates and evaluating protective coatings. It is important in the development and optimization of biosensors and chemical sensors, as well as the analysis of cells and tissues using bioelectrochemistry. In addition, EIS is used to measure capacitance and characterize electrode materials in supercapacitors, optimize electroplating and electrodeposition procedures, and evaluate solar cell performance in photovoltaics. This technique provides in-depth insights into charge transfer, material characteristics, and system dynamics, making it critical for developing innovations in energy storage, corrosion protection, sensing, and bioelectronics [75].

CHAPTER 5: RESULTS AND DISCUSSION

5.1 Analysis of MXene and PPy/MXene Composite

Material analysis of MXene and its composite with polypyrrole is performed by Xray diffraction (XRD), Scanning Electron Microscopy (SEM) and Fourier Transform Infrared Spectroscopy (FTIR).

5.1.1 Xray Diffraction Analysis (XRD)

X-ray diffraction (XRD) was used to examine the structural formation of the samples created. The diffracted intensities were measured from 10° to 80°. Figure 5.1 shows the morphological properties of MAX phase, MXene, and PPy/MXene composite. Ti_3C_2 MXene's diffraction peak (002) at $2\theta = 8.98°$ is shifted to lower angle and indicates a large d spacing of around 0.98 nm, as per the Bragg equation $2d \sin\theta=n\lambda$ and is reported in literature[76].

The pattern of MXene also confirms the disappearance of sharp Ti_3AlC_2 MAX phase peak (104) after etching with hydrofluoric (HF) acid[77]. XRD clearly shows a significant loss in crystallinity and structural order following exfoliation. In other situations, minor amounts of MAX phases were found in the original powders. These do not react, and the full width at half-maximum (FWHM) of their peaks remains constant after the HF treatment. The Polypyrrole (PPy) exhibits large peaks at 2θ equals 11.20°; 25°; and 41° reported in literature [78]. The presence of large peaks indicates the material's amorphous structure as shown in (fig 5.2). XRD pattern of PPy/MXene composite has clearly shown the reinforcement of these peaks with MXene peaks at these specific 2θ angles.

This research demonstrates that the degree of crystallinity of the MXene has a significant impact on the structural features of the composite, thus changing the inherently non-crystalline structure of PPy. Thus, this study has verified the successful development of the PPy/MXene composite, revealing a well-integrated hybrid structure in which the MXene matrix mostly influences the composite's overall crystallinity.
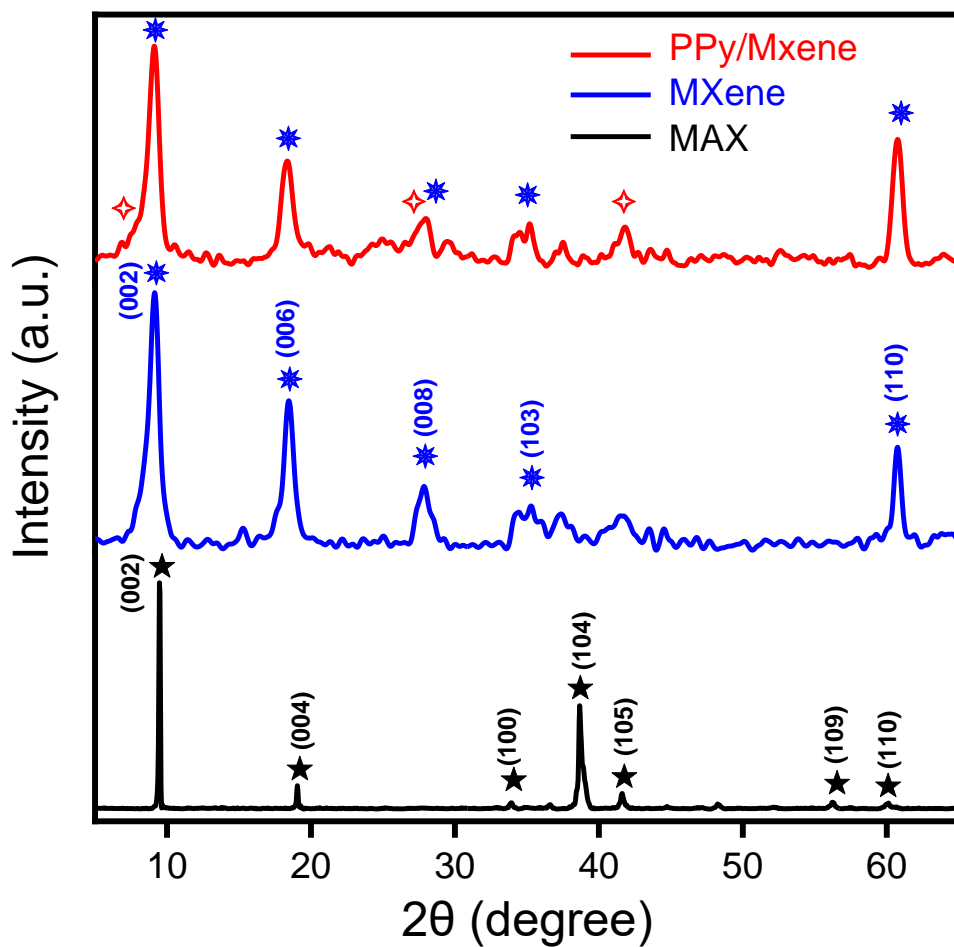
Figure 5.1: XRD plot of MAX phase, MXene and PPy/MXene composite
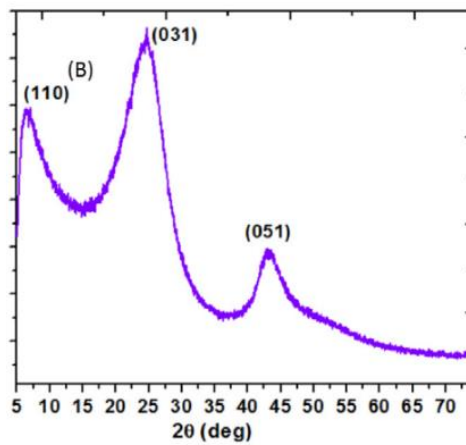
Figure 5.2: XRD of polypyrrole (PPy) from literature[78]

5.1.2 *Scanning Electron Microscopy Analysis (SEM)*

Scanning electron microscopy (SEM) was used to examine the surface morphology of the produced samples. Fig 5.3 shows the morphological features of MAX phase, MXene, PPy/MXene, bare graphite felt, MXene coated graphite felt, and PPy/MXene coated graphite felt. SEM image of the MAX phase reveal its multilayer crystalline structure (fig 5.3a).
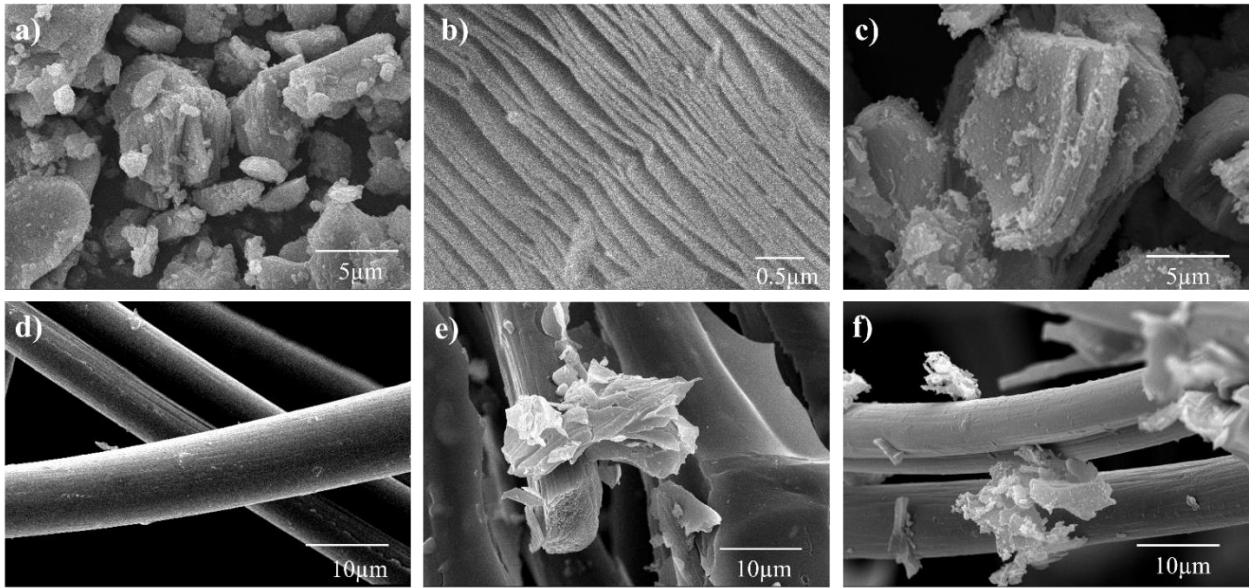
Figure 5.3: SEM images of (a) MAX phase (b) MXene (c) PPy/MXene, (d) Bare GF (e) MXene@GF (f) PPy/MXene@GF

In (Fig 5.3b), the layers are separated, generating an accordion-like shape, which provides evidence of selective etching of Al after the acidic treatment. Two-dimensional MXene and PPy/MXene nanosheets were present in the material to enhance substrate transport and to offer adhesive sites for microbial growth. Additionally, the bioelectrochemical system's microbial enrichment can be modulated by the presence of Ti elements in MXene [54]. Fig 5.3c shows polypyrrole deposition on MXene surface as well as between the layers.

The polypyrrole chains can infiltrate the interlayer spaces of MXene, leading to a composite material with synergistic properties. This integration can improve conductivity,

ion transport kinetics, and stability, making the composite suitable for various electrochemical applications. Fig 5.3d shows a SEM picture of uncoated graphite felt (GF), revealing tiny fibers with a smooth surface. Figures 5.3e and 5.3f show the SEM images of MXene@GF and PPy/MXene@GF. We can see a rougher surface as compared to uncoated GF, proving the coating of MXene and its composite on GF.

5.1.3   Fourier Transform Infrared Spectroscopy (FTIR)

Figure 5.4: FTIR of MXene and PPy/MXene

The FTIR spectra of all the produced samples were compared in the wavenumber range of 4000 cm^{-1} to 500 cm^{-1}, as shown in Figure 5.4. Absorption peaks at 3424 cm^{-1} indicated the existence of hydroxyl groups in both MXene and PPy/MXene samples,

indicating external water, highly hydrogen-bonded OH, or extremely strong coordinated H_2O.

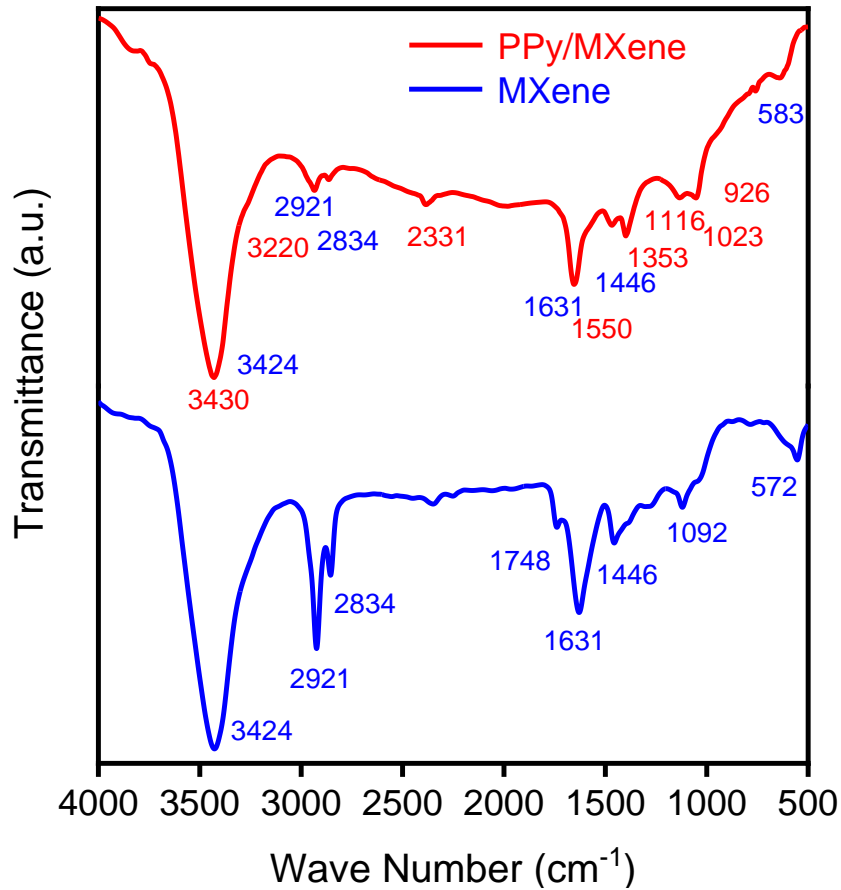The peaks at 572cm^{-1} and 582cm^{-1} were most likely induced by the Ti-O bond's deformation vibration. The classic absorption peak of C=O was seen at 1748 cm^{-1} in MXene and 1631 cm^{-1} in PPy/MXene, with peaks at 2834 cm^{-1} and 2921 cm^{-1} corresponding to C-H stretching in both materials. Peak at 1446cm^{-1} in both samples corresponds to C-F stretching. O-H bending at 1446cm^{-1} is observed in both samples. Peak at 1550cm^{-1} is only found in PPy/MXene composite corresponds to N-O stetching.

Two peaks at 3430cm^{-1} and 3220 cm^{-1} oalso correspond to strong N-H stretching in composite. Furthermore, the peaks at 1550 cm^{-1}, 1353 cm^{-1}, and 1116 cm^{-1} represent the ring stretching vibration, out-of-plane deformation of C-H and stretching and bending of N-C of the PPy/MXene sample. These spectrum patterns highlight the MXene unique structural features and provide compelling evidence of the PPy/MXene composite formation.

5.1.4   Energy Dispersive X-ray Spectroscopy (EDS)

a)

Element	Weight %	MDL	Atomic %
C	27.4	0.16	48.8
N	2.6	0.28	3.9
O	12.6	0.30	16.9
F	6.7	0.13	7.6
Ti	50.7	0.06	22.7

b)

Element	Weight %	MDL	Atomic %
C	19.2	0.43	38.2
O	11.2	0.60	16.7
F	13.7	0.27	17.2
Ti	55.9	0.11	27.9

Figure 5.5: EDX analysis

EDS is frequently used in conjunction with other microscopy techniques, such as Scanning Electron Microscopy (SEM), and it provides elemental analysis capacity, resulting in a thorough understanding of the sample's structure and composition. Fig 5.5 shows EDS results of MXene and PPy/MXene composite. Fig 5.5b shows MXene Ti_3C_2 composition.

It has more concentration of Ti and then C in accordance with formula. Some concentration of O and F is also shown as when MXene gets in contact with air, it becomes functionalized with various functional groups as -O, -F and -OH. Fig 5.5a has clearly exhibited an additional element as N which has further confirmed XRD, SEM and FTIR results as formation of PPy/MXene composite. Additionally, the weight% of C is also enhanced by incorporation of polypyrrole.
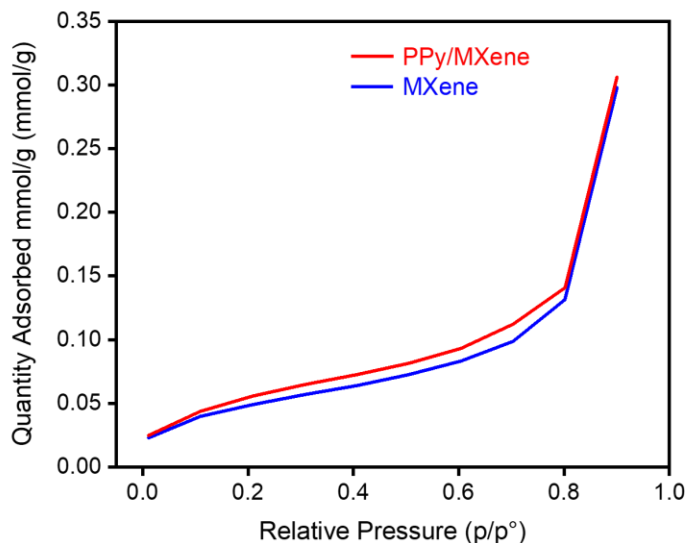
5.1.5   BET Analysis

Figure 5.6: BET Analysis

The physical characteristics of MXene and PPy/MXene composite flakes were analyzed using the N_2 sorption isotherm that was developed through BET experimentation. The specific surface area rose from 3.9304 to 4.4935 (m^2/g) with the addition of polypyrrole in MXene layers and on the surface (Fig 5.6). It may be responsible for the

increased surface area, which leads to a greater number of catalytically active sites. The production of biofilm and MFC performance were both enhanced by the large number of active sites and enhanced surface area.

5.1.6   Contact Angle Measurement

Contact angle of water on bare GF, MXene@GF and PPy/MXene@GF is taken to demonstrate hydrophilicity of materials (Fig 5.7). Pure GF has a hydrophobic surface due to the absence of oxygen-rich groups and hinder bacterial attachment. The -O and -F groups on the surface of MXene@GF make it hydrophilic and angle decreases from 122.43º to 64.42º.
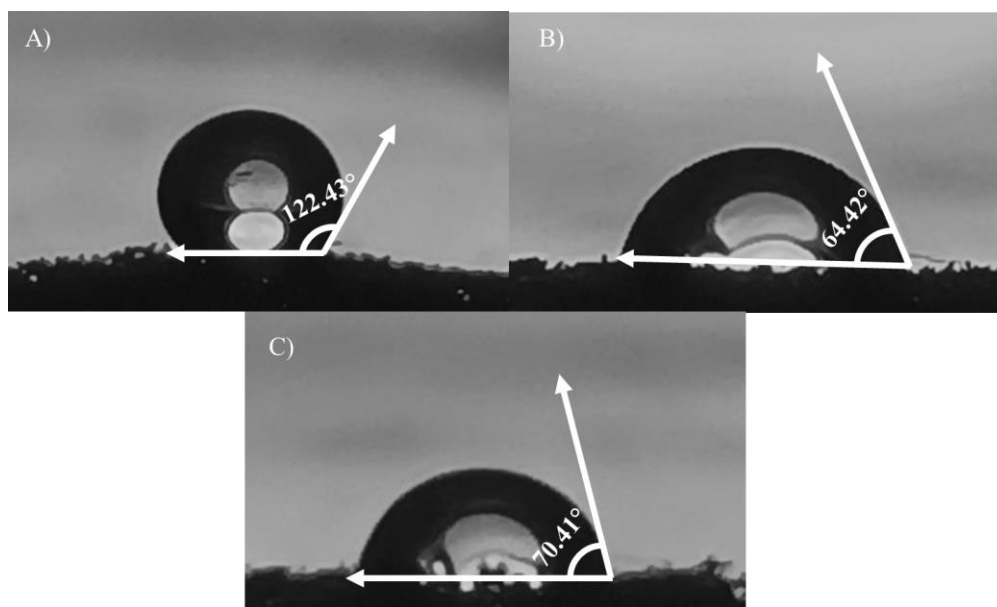
Figure 5.7: Contact Angle Measurement A) Bare GF B) MXene@GF C) PPy/MXene@GF

The water contact angle of PPy/MXene@GF increases somewhat 70.41° compared to MXene@GF due to removal of -O and -F groups during synthesis of composite. While the surface properties remain in the hydrophilic zone, the addition of PPy showed a minor increase in contact angle from 64.42º to 70.41°. In contrast, the GF anode's wettability was significantly improved when contact angle decreased 122.43º to 70.41° for PPy/MXene@GF. Therefore, to encourage microbe attachment and biofilm growth on the

anode surface, covering the GF with the as fabricated PPy/MXene composite catalyst will improve its hydrophilicity.

5.2   Analysis of Microbial Fuel Cells (MFCs)

For determining various properties of MFCs different analysis tools were used as open circuit voltage (OCV), polarizations curves, cyclic voltammetry (CV) and electrochemical impedance spectroscopy (EIS).

5.2.1   *Open Circuit Voltage (OCV) and Electrode Potential*

First, we run the MFCs with the replacement of the solution on a regular basis to get the maximum voltage value. Once the cell has stabilized, we have measured the voltage cycle using an open resistance at a COD concentration of 1000 in the nutritive fluid.

The MFC was first used with sodium acetate as the principal carbon source. We combined the sodium acetate with the nutritious solution to produce a solution with a COD of 1000. Sodium acetate serves as a rapidly biodegradable carbon source for exoelectrogens in MFCs. With each new batch of feed, the electrical voltage output gradually increased. This occurred as the introduced medium adapted to the fuel cell's electrochemically conducting conditions. Once the carbon supply was depleted, the sodium acetate-fed batch's voltage output level dropped abruptly. Fig 5.8 clearly shows that the MFC with PPy/MXene coated graphite felt electrode has the highest OCV value (837 mV), above both the MXene coated graphite felt (753 mV) and the uncoated graphite felt (674 mV). Adding a layer of material to the GF improves conductivity, which leads to greater voltages and better stability.

1000 Ω resistor was connected to find electrode potential. Different cycles were run with load connected externally. (Figure 7A) clearly shows that the MFC with PPy/MXene coated graphite felt electrode has the highest voltage value (281 mV), above both the MXene coated graphite felt (157 mV) and the uncoated graphite felt (101mV). Adding a layer of material to the GF improves conductivity, which leads to greater voltages and better stability.
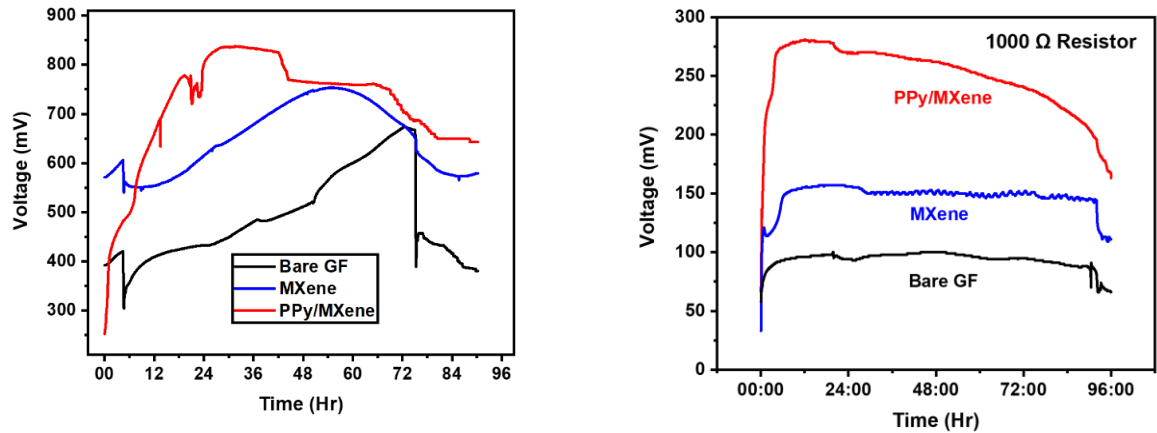
Figure 5.8: Open circuit voltage (OCV) of MFCs and Electrode potential at 1000Ω resistor

5.2.2   *Polarization and Power Density Curves*

Polarization and Power density curves (Fig 5.9) are essential tools for evaluating and understanding the performance of MFCs. These curves plot the cell voltage (V) and power density (mW/m^2) against current density (mA/m^2) providing insights into various elements of MFC operation and performance.

PPy/MXene@GF, MXene@GF, and bareGF MFC had power densities of 264mW/m^2, 197mW/m^2, and 45mW/m^2, respectively, which were 5.86 and 4.37 times greater than the bare GF (45mW/m^2). Increased polarization reduces the MFC's power output. The slope of a point on the polarization curve at a certain current density indicates the degree of polarization at that place. The voltage for polarization cures dropped as current density rose.

The polarization curve of PPy/MXene@GF MFC exhibited the lowest polarization compared to the other MFCs, implying the lowest internal resistance of 50Ω, because at this resistance we obtained the highest power density when compared to MXene@GF and bareGF, which have internal resistances of 250Ω and 1000Ω, respectively. As a result, the MFC with PPy/MXene@GF anode performed better.

59
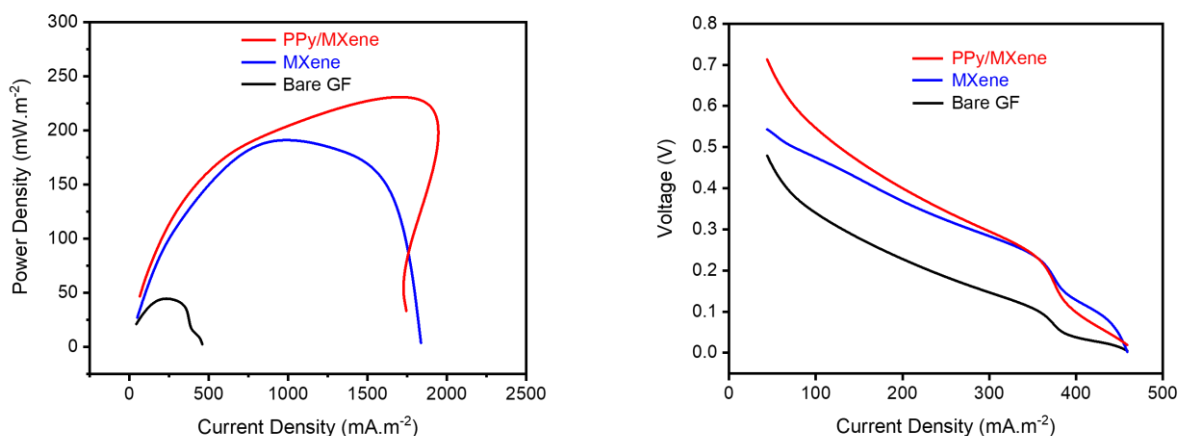
Figure 5.9: Power Density and Polarization Curves

5.2.3 *Cyclic Voltammetry (CV) analysis*

Anode performance was assessed using CV analysis (Fig 5.10). By altering the GF electrode with PPy/MXene and MXene at the scan rate of 100 mV/s, the CV anodic current was greatly improved. (Fig 5.10) illustrates that the electrode with the highest current output was the PPy/MXene@GF (14.3 mA), followed by the electrodes with MXene@GF (9.4 mA), and bare GF (5.2 mA). The closed area of the CV curve can be used to indicate the quantity of electrons transferred at the electrode, reflecting the capacitance of electrode. A larger capacitance would provide more attachment area for microbial and more redox active sites to receive metabolic electrons from an external power source, which is conducive to promoting the EET process [79]. The capacitance can be calculated using the following formula.

$$C_p = \frac{\int_{v_1}^{v_2} i(V)dv}{2A\upsilon(V_2 - V_1)}$$

The V_1 and V_2 are the lowest and highest points of the potential window during CV scanning, i(v) is the instantaneous current, A is the anode surface area (1×1 cm^2), υ is the scanning rate. PPy/MXene electrode exhibited a better capacitance (360 mF/cm^2) compared to the MXene@GF (258 mF/cm^2) and bare GF electrode (124 mF/cm^2), attributed to the superior pseudocapacitive behavior of PPy/MXene@GF over

MXene@GF and bare GF, this was attributed to the increased active sites resulting from the incorporation of PPy in MXene as proved from BET analysis.
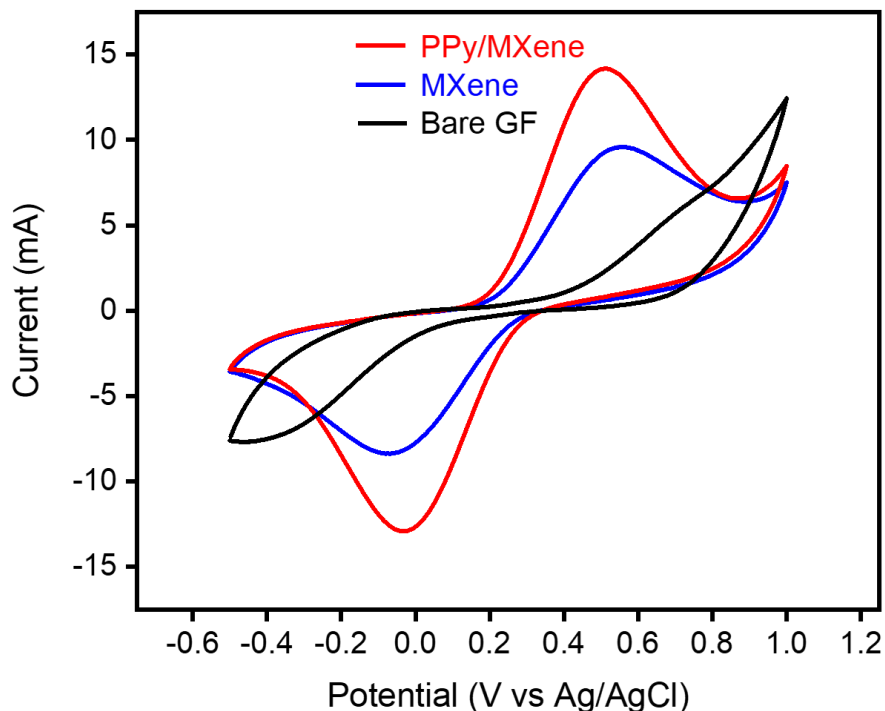
Figure 5.10: CV curves

Furthermore, to establish the bioelectrochemical performance and involvement of microorganisms in EET, both turnover and non-turnover experimental settings were tested (Fig 5.11A) The CV analysis indicates that combining PPy with MXene nanosheets significantly improved the anodic current and electrical conductivity of MXene. PPy/MXene@GF shown improved electrochemical activity for electrogenesis, with much higher electron transfer compared to other electrodes examined.

The catalysts' redox peak in the CV graph was not visible. To identify the peaks, a first derivative analysis of the PPy/MXene@GF and MXene@GF CVs was performed (Fig 5.11B). Various researchers have used CV derivative analysis to show redox peaks that represent anode biofilm activity and species engaged in electron transport.

The derivative was determined by scanning anodic CVs from positive to negative voltage, reflecting potential redox peaks for evaluating electron consumption by microorganisms. Coated electrodes showed strong redox peaks, indicating the presence of b-type and c-type cytochrome involvement in case of MXene@GF while all three types of cytochromes i.e cytochromes a,b and c types aid in electron transmission in case of PPy/MXene@GF.
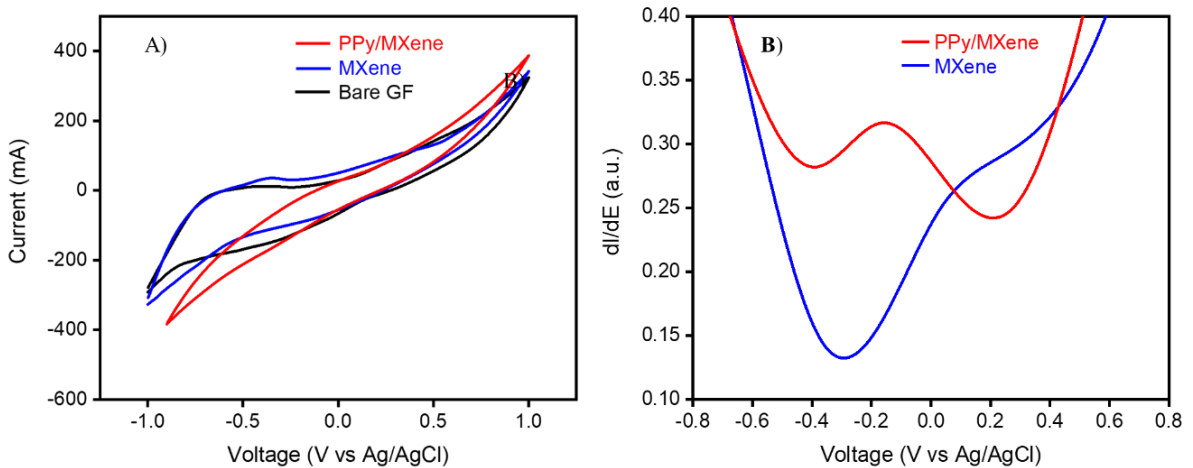
Figure 5.11: CV analysis curves of A) Ref MFC, MXene@GF anode MFC, PPy/MXene@GF anode MFC B) 1st differential curves of CV data of MXene@GF anode MFC, PPy/MXene@GF anode MFC

5.2.4   EIS Analysis (Nyquist Plot)

A Nyquist plot is a graphical representation used in electrochemical impedance spectroscopy (EIS) to show complex impedance data. The graph compares the imaginary (Z'') and real (Z') components of impedance (Z) at various frequencies. The electrocatalytic activity of the PPy/MXene@GF, MXene@GF, and bare GF electrode was evaluated in a typical three-electrode system using EIS (Fig 5.12).

This shows bare GF has more charge transfer resistance (R_{ct}) i.e 179 Ω and solution resistance (R_s) equals 4.23Ω as compared to MXene (R_s=2.20Ω & R_{ct}=24.87Ω) and PPy/MXene (R_s=1.82Ω & R_{ct}=21.23Ω).

62

Thus, PPy/MXene has least charge transfer resistance (R_{ct}) and solution resistance (R_s) which confirms electron transfer is efficient in composite anode also accordance with other results as polarization curve and voltage graphs.

Figure 5.12: Nyquist plots

CHAPTER 6: CONCLUSIONS AND FUTURE RECOMMENDATION

6.1   Conclusion

This study aims to exfoliation of MXene sheets using HF etching method and then formation of MXene/ PPy composite by in-situ polymerization process. Material characterization was done using XRD, SEM, EDX and FTIR analysis. Both samples were coated on Graphite felt (GF) using simple dip and dry coating method.

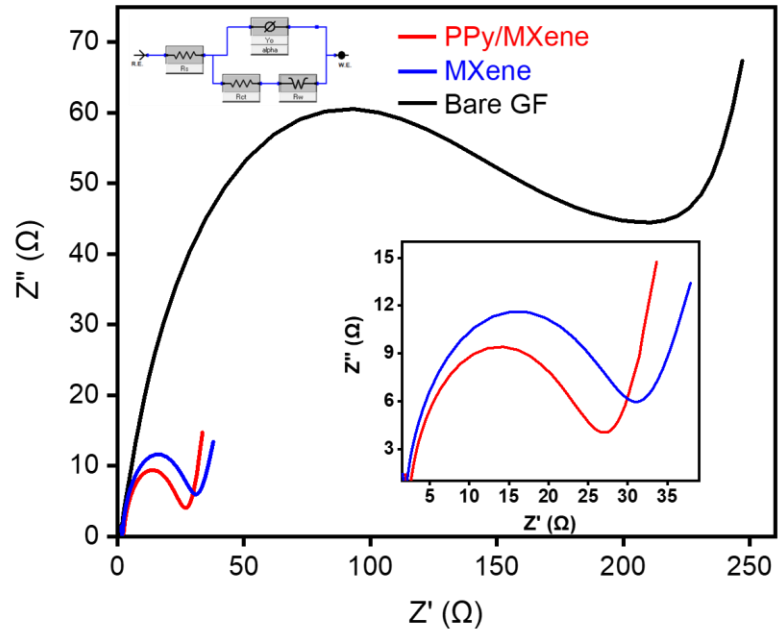Electrochemical experiments showed that PPy/MXene outperformed the other two electrodes in terms of charge transfer resistance and capacitance. The power density of PPy/MXene@GF was found to be 264 mW/m^2, MXene@GF was measured to be 197 mW/m^2 whereas the uncoated/plain graphite felt give the power density of 45 mW/m^2. This study has confirmed increased open circuit voltage (OCV) and power density in the case of PPy/MXene composite anode. This is because charge transfer resistance (R_{ct}) and solution resistance (R_s) are reduced, and comparatively thick biofilm is obtained on PPy/MXene composite anode. This improvement is achieved by facilitating electron transport from microorganisms to the anode as well as allowing microbes to grow in situ at the material's pores. Our findings offer important insights into the use of MXene and its composites in MFC.

6.2   Future Recommendations

There is a requirement for investigation of the use of additional conductive polymers or nanomaterials with MXene to lower charge transfer resistance and increase capacitance. Investigate the impact of various substrate materials and coating processes on the performance of composite electrodes.

As for PPy/MXene composite is concerned, there is need for further exploration of the interactions between various microbial populations and the PPy/MXene composite to better understand the mechanisms underlying improved biofilm development and electron transfer. Experiment with changing the surface characteristics of the PPy/MXene composite to enhance microbial adhesion and growth. Conducting of a cost-benefit

analysis to determine the economic viability of increasing the manufacturing of PPy/MXene composites for commercial use.

By addressing these recommendations, future research can expand on this study's promising results, improving the area of MFCs and the wider application of MXene-based materials in energy and environmental technology.

REFERENCES

1.   Santoro, C., et al., *Microbial fuel cells: From fundamentals to applications. A review.* Journal of power sources, 2017. **356**: p. 225-244.

2.   Badwal, S.P., et al., *Emerging electrochemical energy conversion and storage technologies.* Frontiers in chemistry, 2014. **2**: p. 79.

3.   Liu, H., R. Ramnarayanan, and B.E. Logan, *Production of electricity during wastewater treatment using a single chamber microbial fuel cell.* Environmental science & technology, 2004. **38**(7): p. 2281-2285.

4.   Johnson, J., *Benefits of microbial fuel cell.* AUEssays. https://www. auessays. com/essays/sciences/benefits-microbial-fuel-cell-7067. php, 2018.

5.   Sonawane, A.V., et al., *A review of microbial fuel cell and its diversification in the development of green energy technology.* Chemosphere, 2024: p. 141127.

6.   Rabaey, K., et al., *Microbial ecology meets electrochemistry: electricity-driven and driving communities.* The ISME journal, 2007. **1**(1): p. 9-18.

7.   Logan, B.E., et al., *Microbial fuel cells: methodology and technology.* Environmental science & technology, 2006. **40**(17): p. 5181-5192.

8.   Li, X., et al., *MXene chemistry, electrochemistry and energy storage applications.* Nature Reviews Chemistry, 2022. **6**(6): p. 389-404.

9.   Lei, J.-C., X. Zhang, and Z. Zhou, *Recent advances in MXene: Preparation, properties, and applications.* Frontiers of Physics, 2015. **10**: p. 276-286.

10.   McNeill, R., et al., *Electronic conduction in polymers. I. The chemical structure of polypyrrole.* Australian Journal of Chemistry, 1963. **16**(6): p. 1056-1075.

11. Kim, B.H., I.S. Chang, and G.M. Gadd, *Challenges in microbial fuel cell development and operation.* Applied microbiology and biotechnology, 2007. **76**(3): p. 485-494.

12. Du, Z., H. Li, and T. Gu, *A state of the art review on microbial fuel cells: a promising technology for wastewater treatment and bioenergy.* Biotechnology advances, 2007. **25**(5): p. 464-482.

13. Rabaey, K. and W. Verstraete, *Microbial fuel cells: novel biotechnology for energy generation.* TRENDS in Biotechnology, 2005. **23**(6): p. 291-298.

14. Watanabe, K., *Recent developments in microbial fuel cell technologies for sustainable bioenergy.* Journal of bioscience and bioengineering, 2008. **106**(6): p. 528-536.

15. Logan, B.E., *Microbial fuel cells*. 2008: John Wiley & Sons.

16. Logan, B.E., *Exoelectrogenic bacteria that power microbial fuel cells.* Nature Reviews Microbiology, 2009. **7**(5): p. 375-381.

17. Bond, D.R. and D.R. Lovley, *Electricity production by Geobacter sulfurreducens attached to electrodes.* Applied and environmental microbiology, 2003. **69**(3): p. 1548-1555.

18. Rabaey, K., et al., *A microbial fuel cell capable of converting glucose to electricity at high rate and efficiency.* Biotechnology letters, 2003. **25**: p. 1531-1535.

19. Schröder, U., *From Wastewater to Hydrogen: Biorefineries Based on Microbial Fuel-Cell Technology.* ChemSusChem: Chemistry & Sustainability Energy & Materials, 2008. **1**(4): p. 281-282.

20. Flimban, S.G., et al., *Overview of recent advancements in the microbial fuel cell from fundamentals to applications: Design, major elements, and scalability.* Energies, 2019. **12**(17): p. 3390.

21.   Borja-Maldonado, F. and M.Á.L. Zavala, *Contribution of configurations, electrode and membrane materials, electron transfer mechanisms, and cost of components on the current and future development of microbial fuel cells.* Heliyon, 2022. **8**(7).

22.   Priya, A., et al., *Advancements on sustainable microbial fuel cells and their future prospects: A review.* Environmental Research, 2022. **210**: p. 112930.

23.   Rahimnejad, M., et al., *A review on the effect of proton exchange membranes in microbial fuel cells.* Biofuel Research Journal, 2014. **1**(1): p. 7-15.

24.   Lovley, D.R., *Microbial fuel cells: novel microbial physiologies and engineering approaches.* Current opinion in biotechnology, 2006. **17**(3): p. 327-332.

25.   Oh, S. and B.E. Logan, *Hydrogen and electricity production from a food processing wastewater using fermentation and microbial fuel cell technologies.* Water research, 2005. **39**(19): p. 4673-4682.

26.   Di Lorenzo, M., et al., *A single-chamber microbial fuel cell as a biosensor for wastewaters.* Water research, 2009. **43**(13): p. 3145-3154.

27.   Liu, L., et al., *Double-chamber microbial fuel cells started up under room and low temperatures.* International journal of hydrogen energy, 2013. **38**(35): p. 15574-15579.

28.   Mukherjee, A., et al., *Effective power management system in stacked microbial fuel cells for onsite applications.* Journal of Power Sources, 2022. **517**: p. 230684.

29.   Mehravanfar, H., M.A. Mahdavi, and R. Gheshlaghi, *Economic optimization of stacked microbial fuel cells to maximize power generation and treatment of wastewater with minimal operating costs.* International journal of hydrogen energy, 2019. **44**(36): p. 20355-20367.

30.   He, Z., S.D. Minteer, and L.T. Angenent, *Electricity generation from artificial wastewater using an upflow microbial fuel cell.* Environmental science & technology, 2005. **39**(14): p. 5262-5267.

31. Dewan, A., et al., *Evaluating the performance of microbial fuel cells powering electronic devices.* Journal of power sources, 2010. **195**(1): p. 90-96.

32. Schröder, U., *Anodic electron transfer mechanisms in microbial fuel cells and their energy efficiency.* Physical Chemistry Chemical Physics, 2007. **9**(21): p. 2619-2629.

33. Lovley, D.R., *The microbe electric: conversion of organic matter to electricity.* Current opinion in Biotechnology, 2008. **19**(6): p. 564-571.

34. Marsili, E., et al., *Shewanella secretes flavins that mediate extracellular electron transfer.* Proceedings of the National Academy of Sciences, 2008. **105**(10): p. 3968-3973.

35. Breuer, M., et al., *Multi-haem cytochromes in Shewanella oneidensis MR-1: structures, functions and opportunities.* Journal of The Royal Society Interface, 2015. **12**(102): p. 20141117.

36. Rossi, R., et al., *Quantifying the factors limiting performance and rates in microbial fuel cells using the electrode potential slope analysis combined with electrical impedance spectroscopy.* Electrochimica Acta, 2020. **348**: p. 136330.

37. Zafar, H., et al., *Meta-analysis of operational performance and response metrics of microbial fuel cells (MFCs) fed with complex food waste.* Journal of Environmental Management, 2022. **315**: p. 115152.

38. Mier, A.A., et al., *A review of recent advances in electrode materials for emerging bioelectrochemical systems: From biofilm-bearing anodes to specialized cathodes.* Chemosphere, 2021. **283**: p. 131138.

39. Wang, X., et al., *Use of carbon mesh anodes and the effect of different pretreatment methods on power production in microbial fuel cells.* Environmental science & technology, 2009. **43**(17): p. 6870-6874.

40.   Lai, M.-F., C.-W. Lou, and J.-H. Lin, *Improve 3D electrode materials performance on electricity generation from livestock wastewater in microbial fuel cell.* International Journal of Hydrogen Energy, 2018. **43**(25): p. 11520-11529.

41.   Choudhury, P., et al., *Performance improvement of microbial fuel cell (MFC) using suitable electrode and Bioengineered organisms: A review.* Bioengineered, 2017. **8**(5): p. 471-487.

42.   Chen, J., et al., *Biodegradation of oxytetracycline and electricity generation in microbial fuel cell with in situ dual graphene modified bioelectrode.* Bioresource technology, 2018. **270**: p. 482-488.

43.   Shen, Y., et al., *Carbon nanofibers modified graphite felt for high performance anode in high substrate concentration microbial fuel cells.* The Scientific World Journal, 2014. **2014**.

44.   Prathiba, S., P.S. Kumar, and G. Rangasamy, *Recent advancements on the development of microbial fuel cells: Anode modification and scale-up challenges in upgrading anode electrode.* International Journal of Hydrogen Energy, 2024.

45.   Santoro, C., et al., *Power generation of microbial fuel cells (MFCs) with low cathodic platinum loading.* International journal of hydrogen energy, 2013. **38**(1): p. 692-700.

46.   Cheng, S., H. Liu, and B.E. Logan, *Power densities using different cathode catalysts (Pt and CoTMPP) and polymer binders (Nafion and PTFE) in single chamber microbial fuel cells.* Environmental science & technology, 2006. **40**(1): p. 364-369.

47.   Kim, K.-Y., W. Yang, and B.E. Logan, *Impact of electrode configurations on retention time and domestic wastewater treatment efficiency using microbial fuel cells.* Water research, 2015. **80**: p. 41-46.

48.   Fan, L., J. Shi, and T. Gao, *Comparative study on the effects of three membrane modification methods on the performance of microbial fuel cell.* Energies, 2020. **13**(6): p. 1383.

49.   Banerjee, A., R.K. Calay, and F.E. Eregno, *Role and important properties of a membrane with its recent advancement in a microbial fuel cell.* Energies, 2022. **15**(2): p. 444.

50.   Rago, L., et al., *Influences of dissolved oxygen concentration on biocathodic microbial communities in microbial fuel cells.* Bioelectrochemistry, 2017. **116**: p. 39-51.

51.   Lamiel, C., et al., *Beyond Ti-based MXenes: A review of emerging non-Ti based metal-MXene structure, properties, and applications.* Materials Today, 2023. **63**: p. 313-338.

52.   Chen, J., et al., *Recent progress and advances in the environmental applications of MXene related materials.* Nanoscale, 2020. **12**(6): p. 3574-3592.

53.   Zhan, X., et al., *MXene and MXene-based composites: synthesis, properties and environment-related applications.* Nanoscale Horizons, 2020. **5**(2): p. 235-258.

54.   Liu, D., et al., *Ti 3 C 2 MXene as an excellent anode material for high-performance microbial fuel cells.* Journal of Materials Chemistry A, 2018. **6**(42): p. 20887-20895.

55.   Duchet, J., R. Legras, and S. Demoustier-Champagne, *Chemical synthesis of polypyrrole: structure–properties relationship.* Synthetic metals, 1998. **98**(2): p. 113-122.

56.   Wysocka-Żołopa, M., et al., *Structure and electrochemical properties of magnetite and polypyrrole nanocomposites formed by pyrrole oxidation with magnetite nanoparticles.* Journal of Solid State Electrochemistry, 2023. **27**(7): p. 1919-1934.

57.   Zou, Y., J. Pisciotta, and I.V. Baskakov, *Nanostructured polypyrrole-coated anode for sun-powered microbial fuel cells.* Bioelectrochemistry, 2010. **79**(1): p. 50-56.

58.   Abd Mutalib, M., et al., *Scanning electron microscopy (SEM) and energy-dispersive X-ray (EDX) spectroscopy*, in *Membrane characterization*. 2017, Elsevier. p. 161-179.

59.   Liu, J. and J. Cowley, *High-resolution scanning transmission electron microscopy.* Ultramicroscopy, 1993. **52**(3-4): p. 335-346.

60.   Chatti, S., et al., *CIRP encyclopedia of production engineering*. 2019: Springer.

61.   Mohammed, A. and A. Abdullah. *Scanning electron microscopy (SEM): A review*. in *Proceedings of the 2018 International Conference on Hydraulics and Pneumatics—HERVEX, Băile Govora, Romania*. 2018.

62.   Chatterjee, A., *X-ray diffraction.* Handbook of analytical techniques in concrete science and technology, 2000: p. 275-332.

63.   Painuly, J.P., *Barriers to renewable energy penetration; a framework for analysis.* Renewable energy, 2001. **24**(1): p. 73-89.

64.   Pope, C.G., *X-ray diffraction and the Bragg equation.* Journal of chemical education, 1997. **74**(1): p. 129.

65.   Mohamed, M.A., et al., *Fourier transform infrared (FTIR) spectroscopy*, in *Membrane characterization*. 2017, Elsevier. p. 3-29.

66.   Möllmann, K.-P. and M. Vollmer, *Fourier transform infrared spectroscopy in physics laboratory courses.* European journal of physics, 2013. **34**(6): p. S123.

67.   Bacsik, Z., J. Mink, and G. Keresztury, *FTIR spectroscopy of the atmosphere. I. Principles and methods.* Applied Spectroscopy Reviews, 2004. **39**(3): p. 295-363.

68.   Kelani, K.M., et al., *FTIR combined with chemometric tools (fingerprinting spectroscopy) in comparison to HPLC: which strategy offers more opportunities as*

a green analytical chemistry technique for pharmaceutical analysis. Analytical Methods, 2020. **12**(48): p. 5893-5907.

69.   Harnisch, F. and S. Freguia, *A basic tutorial on cyclic voltammetry for the investigation of electroactive microbial biofilms.* Chemistry–An Asian Journal, 2012. **7**(3): p. 466-475.

70.   Luo, T., et al. *CMOS potentiostat for chemical sensing applications*. in *SENSORS, 2013 IEEE*. 2013. IEEE.

71.   Chooto, P., *Cyclic voltammetry and its applications.* Voltammetry. IntechOpen, 2019: p. 1.

72.   Lazanas, A.C. and M.I. Prodromidis, *Electrochemical impedance spectroscopy─ a tutorial.* ACS Measurement Science Au, 2023. **3**(3): p. 162-193.

73.   Ertuğrul Uygun, H.D. and Z.O. Uygun, *Electrochemical Impedance Spectroscopy (EIS) Principles and Biosensing Applications*, in *Handbook of Nanobioelectrochemistry: Application in Devices and Biomolecular Sensing*. 2023, Springer. p. 919-932.

74.   Magar, H.S., R.Y. Hassan, and A. Mulchandani, *Electrochemical impedance spectroscopy (EIS): Principles, construction, and biosensing applications.* Sensors, 2021. **21**(19): p. 6578.

75.   Chang, B.-Y. and S.-M. Park, *Electrochemical impedance spectroscopy.* Annual Review of Analytical Chemistry, 2010. **3**: p. 207-229.

76.   Salim, O., et al., *Introduction to MXenes: synthesis and characteristics.* Materials Today Chemistry, 2019. **14**: p. 100191.

77.   Naguib, M., et al., *Two-dimensional transition metal carbides.* ACS nano, 2012. **6**(2): p. 1322-1331.

78. Folorunso, O., et al., *Statistical characterization and simulation of graphene-loaded polypyrrole composite electrical conductivity.* Journal of Materials Research and Technology, 2020. **9**(6): p. 15788-15801.

79. Wang, Y., et al., *3D Hierarchical Co_8FeS_8-$FeCo_2O_4$/N-CNTs@ CF with an Enhanced Microorganisms–Anode Interface for Improving Microbial Fuel Cell Performance.* 2022.